



# Engineering a Live Attenuated Porcine Epidemic Diarrhea Virus Vaccine Candidate via Inactivation of the Viral 2'-O-Methyltransferase and the Endocytosis Signal of the Spike Protein

Yixuan Hou,<sup>a,b</sup> Hanzhong Ke,<sup>c</sup> Jineui Kim,<sup>c</sup>  Dongwan Yoo,<sup>c</sup> Yunfang Su,<sup>a,b</sup> Patricia Boley,<sup>a,b</sup> Juliet Chepngeno,<sup>a,b</sup>  Anastasia N. Vlasova,<sup>a,b</sup> Linda J. Saif,<sup>a,b</sup> Qihong Wang<sup>a,b</sup>

<sup>a</sup>Food Animal Health Research Program, Ohio Agricultural Research and Development Center, College of Food, Agriculture and Environmental Sciences, The Ohio State University, Wooster, Ohio, USA

<sup>b</sup>Department of Veterinary Preventive Medicine, College of Veterinary Medicine, The Ohio State University, Wooster, Ohio, USA

<sup>c</sup>Department of Pathobiology, College of Veterinary Medicine, University of Illinois at Urbana-Champaign, Urbana, Illinois, USA

**ABSTRACT** Porcine epidemic diarrhea virus (PEDV) causes high mortality in neonatal piglets; however, effective and safe vaccines are still not available. We hypothesized that inactivation of the 2'-O-methyltransferase (2'-O-MTase) activity of nsp16 and the endocytosis signal of the spike protein attenuates PEDV yet retains its immunogenicity in pigs. We generated a recombinant PEDV, KDKE<sup>4A</sup>, with quadruple alanine substitutions in the catalytic tetrad of the 2'-O-MTase using a virulent infectious cDNA clone, icPC22A, as the backbone. Next, we constructed another mutant, KDKE<sup>4A</sup>-SYA, by abolishing the endocytosis signal of the spike protein of KDKE<sup>4A</sup>. Compared with icPC22A, the KDKE<sup>4A</sup> and KDKE<sup>4A</sup>-SYA mutants replicated less efficiently *in vitro* but induced stronger type I and type III interferon responses. The pathogenesis and immunogenicities of the mutants were evaluated in gnotobiotic piglets. The virulence of KDKE<sup>4A</sup>-SYA and KDKE<sup>4A</sup> was significantly reduced compared with that of icPC22A. Mortality rates were 100%, 17%, and 0% in the icPC22A-, KDKE<sup>4A</sup>-, and KDKE<sup>4A</sup>-SYA-inoculated groups, respectively. At 21 days post-inoculation (dpi), all surviving pigs were challenged orally with a high dose of icPC22A. The KDKE<sup>4A</sup>-SYA- and KDKE<sup>4A</sup>-inoculated pigs were protected from the challenge, because no KDKE<sup>4A</sup>-SYA- and one KDKE<sup>4A</sup>-inoculated pig developed diarrhea whereas all the pigs in the mock-inoculated group had severe diarrhea, and 33% of them died. Furthermore, we serially passaged the KDKE<sup>4A</sup>-SYA mutant in pigs three times and did not find any reversion of the introduced mutations. The data suggest that KDKE<sup>4A</sup>-SYA may be a PEDV vaccine candidate.

**IMPORTANCE** PEDV is the most economically important porcine enteric viral pathogen and has caused immense economic losses in the pork industries in many countries. Effective and safe vaccines are desperately required but still not available. 2'-O-MTase (nsp16) is highly conserved among coronaviruses (CoVs), and the inactivation of nsp16 in live attenuated vaccines has been attempted for several betacoronaviruses. We show that inactivation of both 2'-O-MTase and the endocytosis signal of the spike protein is an approach to designing a promising live attenuated vaccine for PEDV. The *in vivo* passaging data also validated the stability of the KDKE<sup>4A</sup>-SYA mutant. KDKE<sup>4A</sup>-SYA warrants further evaluation in sows and their piglets and may be used as a platform for further optimization. Our findings further confirmed that nsp16 can be a universal target for CoV vaccine development and will aid in the development of vaccines against other emerging CoVs.

**KEYWORDS** 2'-O-methyltransferase, PEDV, vaccine, coronavirus, nsp16

**Citation** Hou Y, Ke H, Kim J, Yoo D, Su Y, Boley P, Chepngeno J, Vlasova AN, Saif LJ, Wang Q. 2019. Engineering a live attenuated porcine epidemic diarrhea virus vaccine candidate via inactivation of the viral 2'-O-methyltransferase and the endocytosis signal of the spike protein. *J Virol* 93:e00406-19. <https://doi.org/10.1128/JVI.00406-19>.

**Editor** Tom Gallagher, Loyola University Chicago

**Copyright** © 2019 American Society for Microbiology. All Rights Reserved.

Address correspondence to Qihong Wang, wang.655@osu.edu.

**Received** 7 March 2019

**Accepted** 13 May 2019

**Accepted manuscript posted online** 22 May 2019

**Published** 17 July 2019

Porcine epidemic diarrhea virus (PEDV) is a member of the genus *Alphacoronavirus* within the family *Coronaviridae*. Its ~28-kb genomic RNA (gRNA) contains six known open reading frames, encoding the replicase polyproteins (pp1a and pp1ab), four structural proteins (spike [S], envelope [E], membrane [M], and nucleocapsid [N]), and an accessory protein (ORF3). The glycoprotein S mediates receptor binding and membrane fusion during virus entry and harbors major viral neutralizing epitopes. PEDV classical strains (genogroup 1 [G1]) emerged in the United Kingdom in 1971 and caused endemic outbreaks in many European and Asian countries. In 2010, highly virulent PEDV strains (G2) emerged in China, and these viruses have since spread to North America, Europe, and other Asian countries and have caused epidemic outbreaks, resulting in massive mortality in neonatal piglets (1–3). PEDV was first detected in U.S. swine in 2013 and caused the death of 7 million pigs within 1 year, leading to \$0.9 to \$1.8 billion in economic losses (4, 5).

To prevent and control the deadly disease, the U.S. Department of Agriculture has conditionally licensed two PEDV vaccines. One is a viral vector-based S subunit vaccine (Harrivaccines Inc. [acquired by Merck & Co.]), and the other is an inactivated vaccine (Zoetis Inc.). Nevertheless, the efficacies of these vaccines remain questionable (6–8). Together with knowledge about vaccines for other swine enteric viruses, such as rotavirus and transmissible gastroenteritis virus (TGEV) (9, 10), oral immunization of sows with a live attenuated vaccine (LAV) is a promising approach to protect newborn piglets against the highly virulent PEDV. PEDV LAVs based on classical (G1) strains have been applied in Asian countries (11), but their efficacies against the emerging highly virulent (G2) strains were minimal, probably due to the antigenic difference between the S proteins of G1 and G2 strains (12). To develop G2 PEDV LAVs, we and other research groups have previously applied the traditional method of attenuation via serially passaging virulent G2 isolates in Vero cells (13–20). Although these LAV candidates were attenuated sufficiently in pigs, they usually failed to consistently induce adequate protective immunity against challenge with the virulent G2 strains (16, 20). One potential reason is that multiple mutations have accumulated in the S genes of the Vero cell-adapted PEDVs (14, 21). These mutations may alter the antigenicity of the S proteins and impair viral immunogenicity *in vivo*, leading to decreased efficacy. Therefore, a better strategy for PEDV LAVs should be to maintain the critical epitopes in the S protein that are conserved in the wild-type viruses to retain optimal immunogenicity. The major concern for LAVs is the safety issue caused by point mutations and recombination in the field. Therefore, the PEDV LAV should harbor rationally introduced mutations in multiple locations in the viral genome to reduce the potential for reversion to virulence. Such a vaccine candidate can be generated using an infectious cDNA clone of a virulent PEDV strain (22).

Similar to those of other coronaviruses (CoVs), the PEDV replicase polyproteins are processed into 16 nonstructural proteins (nsps) that are responsible for viral replication, transcription, translation, etc. The 5' end of each viral genomic RNA and subgenomic mRNA (sgmRNA) contains cap structures: an N-7 methylated guanosine nucleoside (m7GpppN) (cap 0) and a methyl group at the 2'-O-ribose position (cap 1) of the first nucleotide. These cap structures are critical for the effective translation of viral proteins and evasion of host innate immunity (24, 25). Methylation of the two sites in the 5' cap are catalyzed by three nsps, nsp14 (the N-7 methyltransferase [MTase] domain), nsp16 (the 2'-O-MTase), and nsp10 (26–30). CoV nsp16 contains a catalytic tetrad (amino acid residues K, D, K, and E) that is directly responsible for its enzymatic activity (27, 31). Inactivation of nsp16 has been demonstrated to be an effective approach to rationally design LAV candidates for CoVs, since this viral protein is highly conserved among CoVs, and the recombinant viruses carrying mutations in nsp16 are usually viable. It has been documented that introduction of a D130A substitution into the nsp16 of severe acute respiratory syndrome CoV (SARS-CoV) (32) and Middle East respiratory syndrome CoV (MERS-CoV) (33) or an equivalent D129A substitution into mouse hepatitis virus (MHV) (34) attenuated these CoVs in mice. A subsequent study also demonstrated that inactivation of both nsp16 and the exonuclease domain of

nsp14 further attenuated SARS-CoV in mice, with increased genetic stability (35). Moreover, primary infection with the recombinant SARS-CoV fully protected mice from lethal challenge with virulent virus, suggesting that a CoV with its 2'-O-MTase abolished could be a universal LAV platform for additional mutations.

In this study, we applied this knowledge to PEDV to generate and evaluate an LAV platform using the virulent PEDV infectious cDNA clone icPC22A as the backbone (22). PEDV mutants with nsp16 inactivated were generated, with partial (D129A) or complete (KDKE<sup>4A</sup>) replacement of the catalytic tetrad. To achieve a higher level of attenuation and reduce the potential for reversion, we inactivated the endocytosis signal in the cytoplasmic tail of the S protein of KDKE<sup>4A</sup> and generated KDKE<sup>4A</sup>-SYA. We demonstrated previously that inactivation of the endocytosis signal partially attenuated the virulent icPC22A in neonatal piglets without altering major neutralizing epitopes (36). Lack of this signal also caused more S proteins to be transported to the cell surface, potentially leading to improved recognition of the PEDV mutant by the host immune system. In the present study, we evaluated the virulence, immunogenicity, and genetic stability of KDKE<sup>4A</sup> and KDKE<sup>4A</sup>-SYA mutants in neonatal gnotobiotic (Gn) pigs. We also characterized their ability to trigger interferon (IFN) responses *in vitro*.

## RESULTS

**Generation of PEDV mutants.** Structural and biochemical studies of SARS-CoV nsp16 revealed that replacement of each residue in the catalytic tetrad K<sub>46</sub>-D<sub>130</sub>-K<sub>170</sub>-E<sub>203</sub> with alanine significantly inactivated 2'-O-MTase activity (27, 31). First, we modeled the 3-dimensional (3D) structure of PEDV nsp16 and found that the putative catalytic tetrad K<sub>45</sub>-D<sub>129</sub>-K<sub>169</sub>-E<sub>202</sub> is highly homologous to the counterpart in SARS-CoV (Fig. 1B and C). Next, we introduced a single alanine substitution (D129A) or quadruple alanine substitutions (K45A-D129A-K169A-E202A [designated the KDKE<sup>4A</sup> mutant]) into the catalytic tetrad of the 2'-O-MTase of icPC22A to generate two recombinant PEDV mutants (Fig. 1A). Finally, a third mutant, KDKE<sup>4A</sup>-SYA, was constructed by inactivating both K-D-K-E and the endocytosis signal (Y1378A) of the S protein (Fig. 1D). All three nsp16 mutants (D129A, KDKE<sup>4A</sup>, and KDKE<sup>4A</sup>-SYA) were rescued in Vero cells. Supernatants containing the rescued viruses were harvested (passage 0 [P0]), and single clones of each mutant were purified by plaque assay. The complete genomic sequence of each PEDV mutant was verified by Sanger sequencing.

**Inactivation of 2'-O-MTase decreased viral replication and antagonism to IFN- $\beta$  pretreatment in Vero cells.** We characterized the phenotypes of the recombinant PEDVs in Vero cells. In the growth curves (Fig. 2A and B), the D129A mutant replicated similarly to the virulent icPC22A, including similar peak infectious titers (Fig. 2C). The D129A mutant and icPC22A also formed plaques of similar size (Fig. 2D). In contrast, KDKE<sup>4A</sup> and KDKE<sup>4A</sup>-SYA replicated to significantly lower peak titers than icPC22A ( $P < 0.05$ ). As we demonstrated previously, the SYA mutation (Y1378A in the S gene) enhanced the ability of the mutant icYA to induce cell-cell fusion and produce large plaques (36). Thus, the KDKE<sup>4A</sup>-SYA mutant produced larger plaques and replicated more efficiently at early time points than the KDKE<sup>4A</sup> mutant. It has also been documented that the SARS-CoV and MERS-CoV nsp16 mutants were more sensitive to IFN- $\beta$  responses in cell culture than the wild-type viruses (32, 33). We compared the replication of the recombinant PEDVs in Vero cells that were pretreated with different concentrations of IFN- $\beta$  (Fig. 2E). IFN- $\beta$  pretreatment inhibited the replication of icPC22A in a dose-dependent manner. Although all the nsp16 mutants produced significantly lower titers of progeny viruses than the virulent icPC22A, the KDKE<sup>4A</sup> and KDKE<sup>4A</sup>-SYA mutants were more sensitive to higher concentrations of IFN- $\beta$  than the D129A mutant. Since the mutation Y1378A is located in the transcriptional regulatory sequence (TRS) of ORF3 (Fig. 1D), the subgenomic mRNA-3 (sgmRNA-3) levels in the icYA- and KDKE<sup>4A</sup>-SYA-infected Vero cells were about one log<sub>10</sub> unit lower than that in the icPC22A-infected cells (Fig. 2G).

**D129A, KDKE<sup>4A</sup>, and KDKE<sup>4A</sup>-SYA mutants induced stronger IFN responses than icPC22A *in vitro*.** Recent studies have highlighted the fact that type III IFNs,

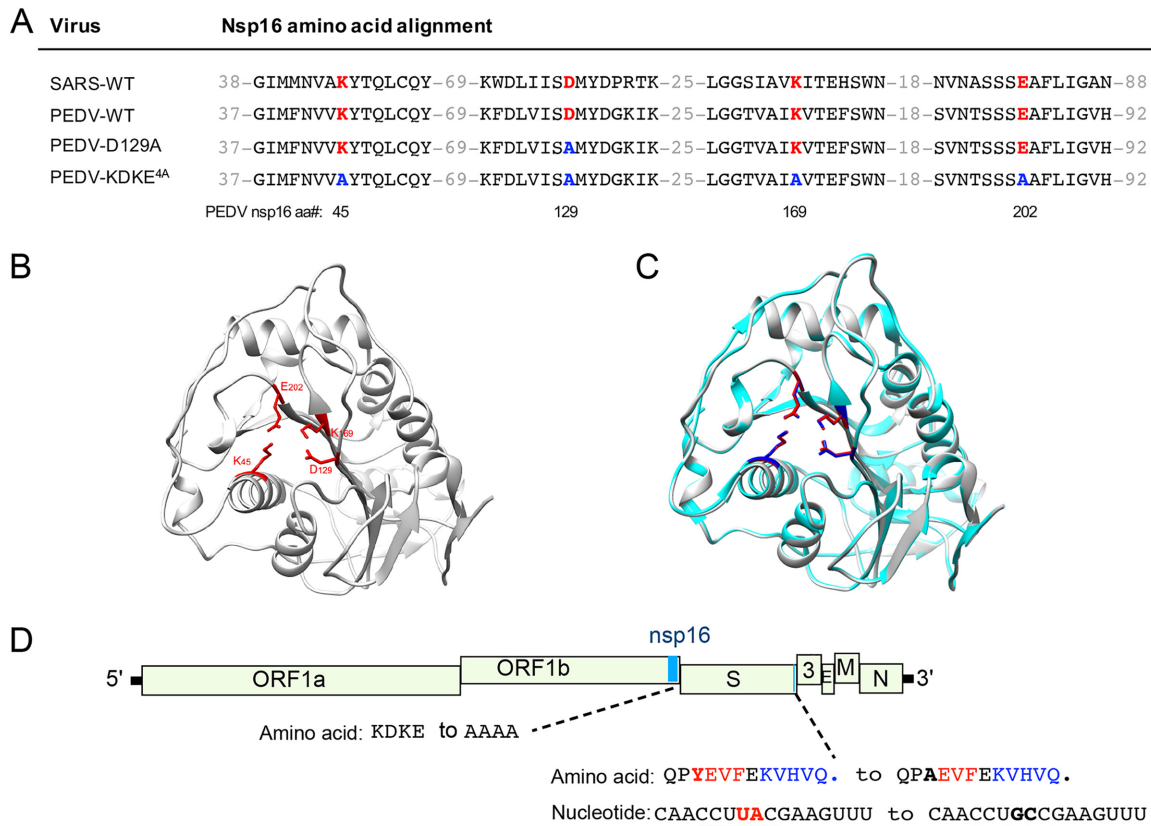


**FIG 1** (A) Alignment of partial amino acids of nsp16 among wild-type (WT) SARS-CoV (SARS-WT), WT PEDV (PEDV-WT), and PEDV mutants (PEDV-D129A and PEDV-KDKE<sup>4A</sup>). The catalytic tetrad KDKE residues are in red. The introduced alanine substitutions are shown in blue. The numbers in gray indicate how many residues in nsp16 are not shown. (B) 3D model of the structure of PEDV nsp16. Residues of the putative catalytic tetrad are shown in red. (C) 3D structure alignment of SARS-CoV nsp16 (cyan) and PEDV nsp16 (gray). The KDKE residues of SARS-CoV are shown in blue, and those of PEDV are shown in red. (D) Diagram of introduced mutations in the KDKE<sup>4A</sup>-SYA mutant. In the amino acid sequence, the motif YEVF is in red and the motif KVHVQ is in blue. The mutated amino acids or nucleotides are in bold. The stop codon in the S protein is indicated as a dot. The predicted 6-nucleotide TRS of ORF3 is underlined.

including IFN- $\lambda$ 1, - $\lambda$ 3, and - $\lambda$ 4, play a significant role in inhibiting PEDV infection *in vitro* (37, 38). It has also been reported that the MHV nsp16 D129A mutant induced stronger IFN- $\beta$  production than the wild-type virus in murine macrophages (34). To evaluate whether the nsp16-inactivated PEDV mutants triggered enhanced type I and type III IFN responses in infected cells, we infected a swine intestinal epithelial cell line (IPEC-DQ) with icPC22A, UV-inactivated icPC22A, or the PEDV mutants at a multiplicity of infection (MOI) of 1. The cells were mock treated or transfected with poly(I-C) as the negative and positive controls. The growth curve analysis showed that the KDKE<sup>4A</sup> and KDKE<sup>4A</sup>-SYA mutants replicated to significantly lower titers than the other viruses at 9 and 12 h postinoculation (hpi) (Fig. 3A). We quantified the mRNAs of swine IFN- $\alpha$ , - $\beta$ , - $\lambda$ 1, - $\lambda$ 3, and - $\lambda$ 4 in the infected cells (Fig. 3B to F). Compared with the virulent icPC22A, the D129A, KDKE<sup>4A</sup>, KDKE<sup>4A</sup>-SYA, and icYA mutants induced significantly higher mRNA levels of all the IFNs at 9 and 12 hpi. The UV-inactivated icPC22A did not stimulate IFN responses. Next, we performed luciferase assays to examine whether infection with the mutant PEDVs activated the IFN- $\lambda$ 1 and - $\beta$  promoters at 9 and 12 hpi (Fig. 3G and H). The IFN promoters were not activated in the icPC22A-infected or mock-treated cells. However, the D129A, KDKE<sup>4A</sup>, and KDKE<sup>4A</sup>-SYA mutants activated the IFN- $\lambda$ 1 and - $\beta$  promoters and induced significantly stronger luciferase activities in IPEC-DQ cells than icPC22A ( $P < 0.05$ ). Collectively, these data suggest that the PEDV D129A, KDKE<sup>4A</sup>, and KDKE<sup>4A</sup>-SYA mutants triggered stronger type I and type III IFN production in infected cells than the virulent PEDV icPC22A.

**KDKE<sup>4A</sup> and KDKE<sup>4A</sup>-SYA mutants were attenuated to different extents in neonatal piglets.** Compared with the D129A single mutant, the KDKE<sup>4A</sup> and KDKE<sup>4A</sup>-

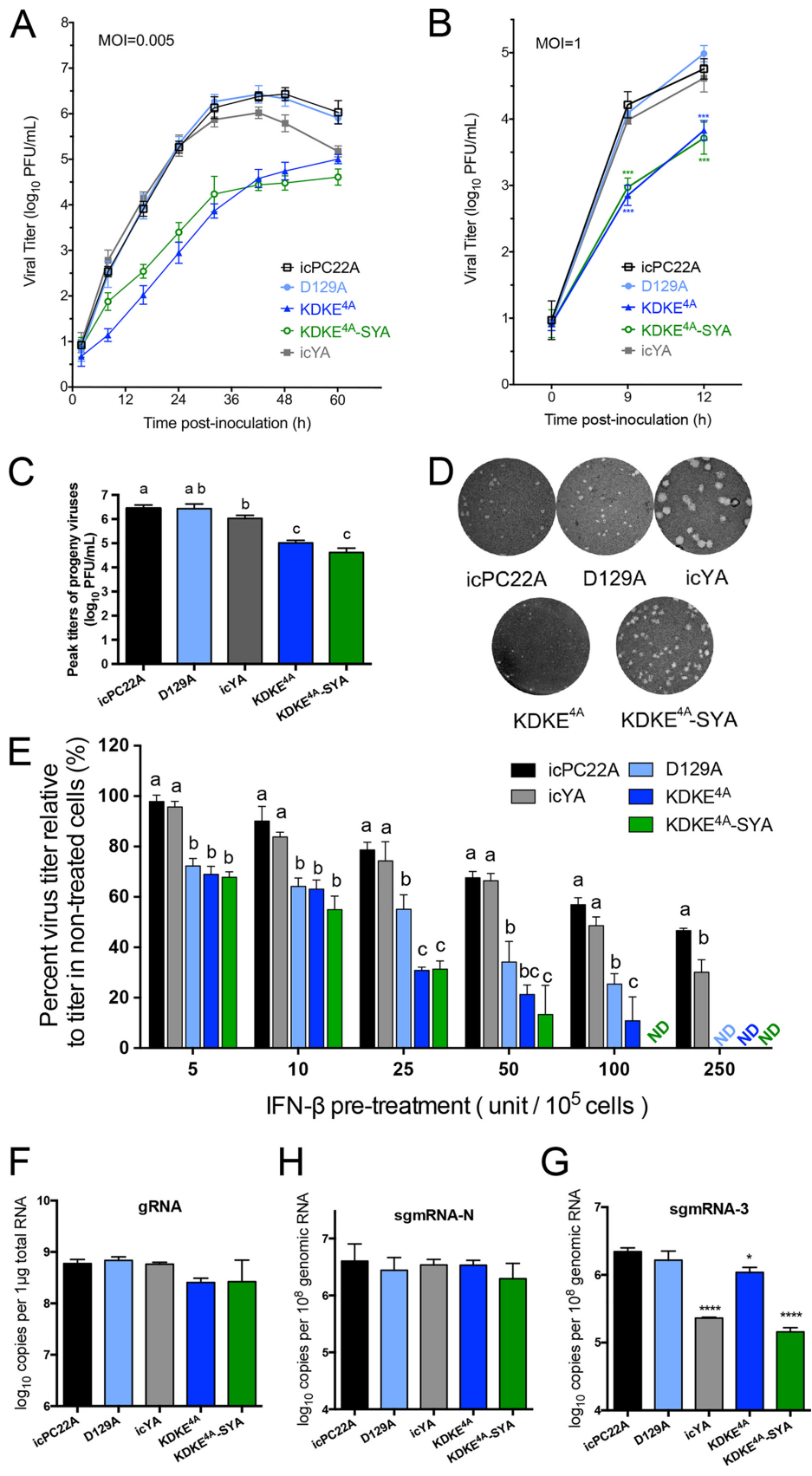


**FIG 2** Growth kinetics, plaque sizes, and sensitivity to IFN-β pretreatment of recombinant PEDVs in Vero cells. (A and B) Growth curves of recombinant PEDVs in Vero cells at MOI of 0.005 (A) and 1 (B). (C) Peak titers of each (Continued on next page)

SYA mutants replicate less effectively and are more sensitive to IFN- $\beta$  responses *in vitro*. We investigated their pathogenesis and immunogenicity in neonatal Gn piglets. In the first 16 days postinoculation (dpi), no clinical signs or mortality was observed for pigs in the mock-inoculated group (Table 1). All eight icPC22A-inoculated piglets had severe diarrhea and died within 6 dpi (100%; 8/8). All KDKE<sup>4A</sup>-inoculated piglets had severe diarrhea, and one piglet died at 10 dpi (16.7%; 1/6). In comparison, only one KDKE<sup>4A</sup>-SYA-inoculated piglet had severe diarrhea for 1 day, and no pigs died (Fig. 4A). The KDKE<sup>4A</sup>- and KDKE<sup>4A</sup>-SYA-infected piglets had significantly lower and delayed peak infectious PEDV shedding titers than the virulent-icPC22A-inoculated pigs ( $2.12 \pm 1.96$  and  $3.24 \pm 1.94$  versus  $5.44 \pm 0.82$  PFU/ml;  $P < 0.05$ ) (Table 1). No significant differences were observed in the amounts of infectious PEDV in the rectal swabs (Fig. 4C) and intestinal contents (Fig. 4E) between KDKE<sup>4A</sup>- and KEKE<sup>4A</sup>-SYA-inoculated pigs at the same time point. The IFN- $\alpha$  levels in the sera collected from the two pigs euthanized at 2 dpi did not differ significantly among the three groups (Fig. 4F). PEDV N proteins were visualized in the epithelial cells of the jejunum and ileum in PEDV-inoculated piglets using immunohistochemistry (IHC) staining (Fig. 5A). The severity of villous atrophy in the infected pigs was quantified by measuring the ratio between villus height and crypt depth (VH/CD ratio) of each villus. The two mutants induced significantly milder villous atrophy in the jejunum and ileum than icPC22A, and the KDKE<sup>4A</sup>-SYA mutant induced significantly milder villous atrophy in the ileum than the KDKE<sup>4A</sup> mutant (Fig. 5B) ( $P < 0.05$ ). Collectively, these data suggest that the inactivation of the catalytic tetrad K-D-K-E in the nsp16 protein significantly attenuated the highly virulent PEDV in neonatal piglets, and the additional inactivation of the endocytosis signal in the S protein further reduced its virulence.

**The KDKE<sup>4A</sup> and KDKE<sup>4A</sup>-SYA mutants induced protection against virulent icPC22A challenge in pigs.** At 21 dpi, the surviving pigs were challenged with the highly virulent icPC22A at a high dose ( $10^6$  PFU/pig) (Table 2). No mortality was observed in the KDKE<sup>4A</sup>- and KDKE<sup>4A</sup>-SYA-inoculated groups, whereas two mock-challenged pigs died 6 or 7 days postchallenge (dpc) (Fig. 6A). By 9 dpc, no KDKE<sup>4A</sup>-SYA-inoculated pig had diarrhea and only one KDKE<sup>4A</sup>-inoculated pig had mild diarrhea for 1 day. However, all the mock-challenged pigs developed severe diarrhea for  $7.17 \pm 0.98$  days (Table 2 and Fig. 6B). No infectious PEDV was detected in the rectal swab samples from pigs in the KDKE<sup>4A</sup>-SYA-inoculated group, and only one sample from one pig in the KDKE<sup>4A</sup>-inoculated group was PEDV positive for 1 day, with a low infectious titer of  $0.22 \log_{10}$  PFU/ml. However, all the mock-challenged pigs shed high titers of infectious PEDV in the feces from 2 to 4 dpc (Fig. 6C). In fecal PEDV RNA-shedding profiles, the trend of the RNA shedding in the KDKE<sup>4A</sup> and KDKE<sup>4A</sup>-SYA groups did not change significantly. In contrast, the mock-challenged pigs shed significantly higher titers of infectious PEDV from 2 to 4 dpc and viral RNA from 2 to 9 dpc than the KDKE<sup>4A</sup> and KDKE<sup>4A</sup>-SYA groups ( $P < 0.05$ ). We also determined the viral neutralizing (VN) antibody titers in the sera collected at 14 dpi/–7 dpc, 21 dpi/0 dpc, and 30 dpi/9 dpc (Fig. 6E). Primary infection of the two PEDV mutants in piglets elicited VN antibodies before challenge, and the challenge significantly boosted titers at 30 dpi/9 dpc, which were significantly higher than those of the mock-challenged pigs ( $P < 0.05$ ). In summary, infection with KDKE<sup>4A</sup> and KDKE<sup>4A</sup>-SYA of 4-day-old piglets induced 80% and 100% protection, respectively, against diarrhea following subsequent challenge with virulent icPC22A.

## FIG 2 Legend (Continued)

recombinant PEDV within 60 hpi in the multistep growth curve (MOI = 0.005). (D) Plaques of recombinant PEDVs in Vero cells. The cells were fixed and stained at 50 hpi. (E) Sensitivities of recombinant PEDVs to IFN- $\beta$  pretreatment in Vero cells. The cells were pretreated with different concentrations of IFN- $\beta$  and inoculated with the individual viruses. ND, nondetectable. (F to H) Real-time RT-qPCR quantification of PEDV genomic RNA (F), sgRNA-N (H), and sgRNA-3 (G) in PEDV-infected Vero cells at 10 hpi. (C and E) Groups with significant differences ( $P < 0.05$ ) are indicated with different letters. (B, F, H, and G) Groups that were significantly different from the icPC22A group are indicated with asterisks (\*,  $P < 0.05$ ; \*\*,  $P < 0.01$ ; \*\*\*,  $P < 0.005$ ; \*\*\*\*,  $P < 0.001$ ). The error bars indicate standard deviations.

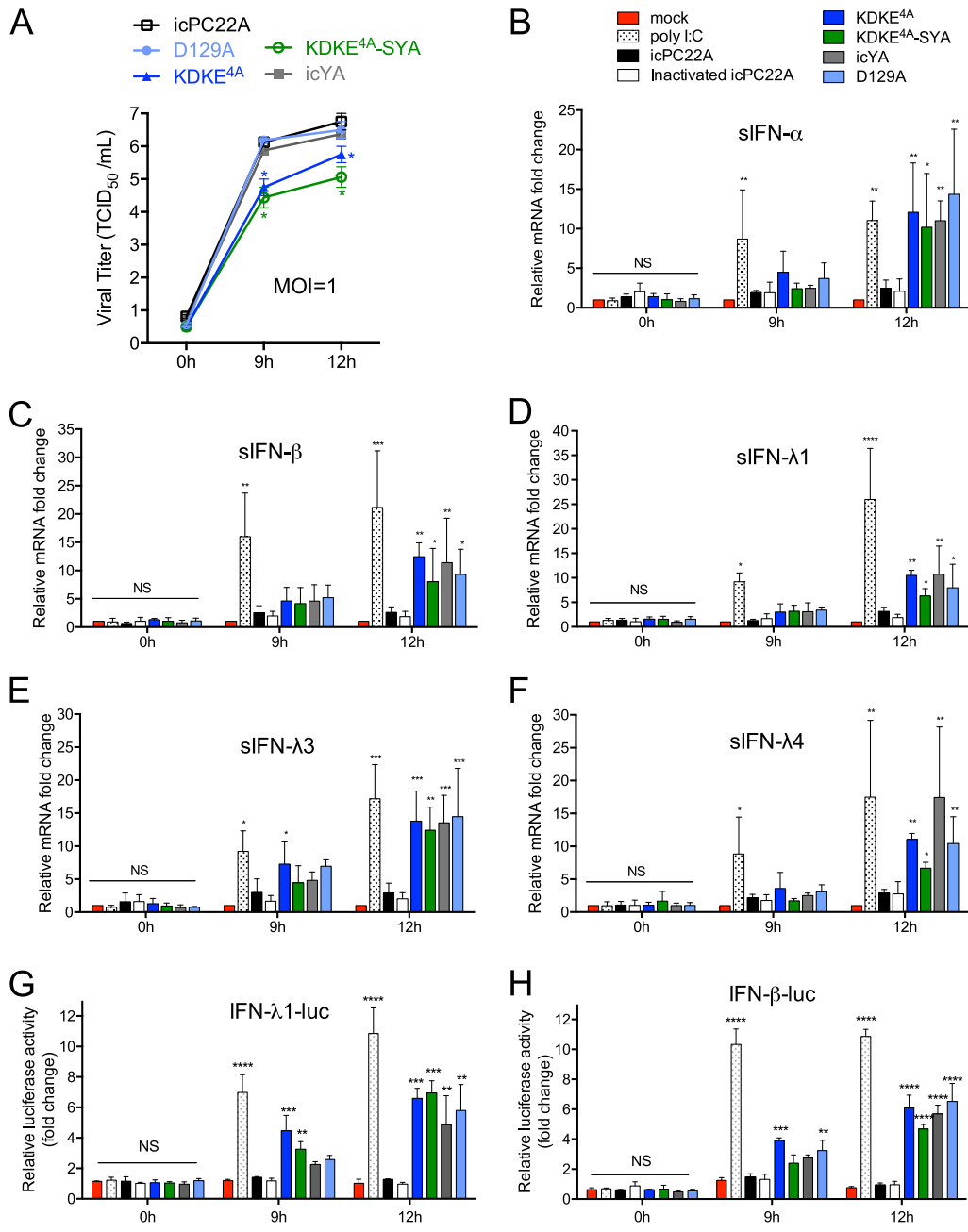


**FIG 3** Induction of type I and type III IFN mRNAs by recombinant PEDVs in the swine intestinal epithelial cell line IPEC-DQ. (A) Growth curves of recombinant PEDVs in IPEC-DQ cells (MOI = 1). (B to F) Relative cellular mRNA levels of swine IFN- $\alpha$ , IFN- $\beta$ , IFN- $\lambda$ 1, IFN- $\lambda$ 3, and IFN- $\lambda$ 4. IPEC-DQ cells were inoculated with recombinant PEDVs (MOI = 1) or UV-inactivated icPC22A, mock treated, or stimulated with poly(I:C). Total RNA was extracted at 0, 9, and 12 hpi and quantified by reverse transcription followed by real-time qPCR. The values are fold changes compared with mock treatment using the  $2^{-\Delta\Delta CT}$  method. (G and H) Activation of the IFN- $\beta$  promoter (G) and IFN- $\lambda$ 1 promoter (H) in IPEC-DQ cells by recombinant PEDVs was quantified by luciferase reporter assays. At each time point, groups with significant differences were analyzed by one-way ANOVA followed by Dennett's test by comparing each group with icPC22A (\*,  $P < 0.05$ ; \*\*,  $P < 0.01$ ; \*\*\*,  $P < 0.005$ ; \*\*\*\*,  $P < 0.001$ ; NS, not significant). The error bars indicate standard deviations.

**The introduced mutations in the KDKE<sup>4A</sup>-SYA mutant were stable after passaging three times in pigs.** The reversion to virulence of an LAV represents a safety concern for its use in livestock. The KDKE<sup>4A</sup>-SYA mutant harbors 11 nucleotide substitutions in its genome and induced 100% protection in neonatal pigs. We evaluated the genetic stability of the introduced mutations by serially passaging the virus in pigs three times (Fig. 7). The viral genome in the intestinal contents at the third passage was

**TABLE 1** Summary of clinical signs and PEDV shedding in Gn piglets after PEDV inoculation (1 to 12 dpi)

Group	No. of pigs	Mortality rate [% (no./total)] <sup>a</sup>	Severe diarrhea rate <sup>b</sup> [% (no./total)]	Onset of diarrhea (dpi)	Duration (days) of severe diarrhea (FC <sup>b</sup> = 3)	Duration (days) of diarrhea (FC <sup>b</sup> ≥ 2)	Peak mean fecal infectious		Peak mean fecal PEDV RNA shedding titer (log <sub>10</sub> copies/ml); dpi
							PEDV shedding titer (log <sub>10</sub> PFU/ml); dpi	RNA shedding titer (log <sub>10</sub> copies/ml); dpi	
iPC22A	8	100 (8/8) <sup>A</sup> <sup>c</sup>	100 (8/8) <sup>A</sup>	1.00 ± 0.00B	NA (>3)	NA (>3)	5.44 ± 0.82A; 1	12.03 ± 0.55A; 1	
KDKE <sup>4A</sup>	8	17 (1/6) <sup>B</sup>	100 (8/8) <sup>A</sup>	2.00 ± 0.65A	3.33 ± 2.34A	10.5 ± 1.38A	2.12 ± 1.96B; 1.5	9.82 ± 1.38B; 1.5	
KDKE <sup>4A</sup> -SYA	7	0 (0/5) <sup>C</sup>	14 (1/7) <sup>B</sup>	1.57 ± 0.19A	0.20 ± 0.45B	8.40 ± 0.89B	3.24 ± 1.94B; 1.5	11.08 ± 1.30AB; 1.5	
Mock	7	0 (0/6) <sup>C</sup>	0 (0/7) <sup>C</sup>	NA <sup>d</sup>	0.00 ± 0.00B	0.00 ± 0.00C	NA	NA	

<sup>a</sup>Two diarrheic piglets from the KDKE<sup>4A</sup> and KDKE<sup>4A</sup>-SYA groups and one mock-treated piglet were euthanized at 2 dpi for histopathological examination and were excluded from calculation of the mortality rate.

<sup>b</sup>Fecal consistency (FC) was scored as follows: 0, solid; 1, pasty; 2, semiliquid; and 3, liquid. FC scores of 2 and 3 were considered moderate diarrhea and severe diarrhea, respectively.

<sup>c</sup>Different letters denote significant differences between groups (*P* < 0.05).

<sup>d</sup>NA, not available.

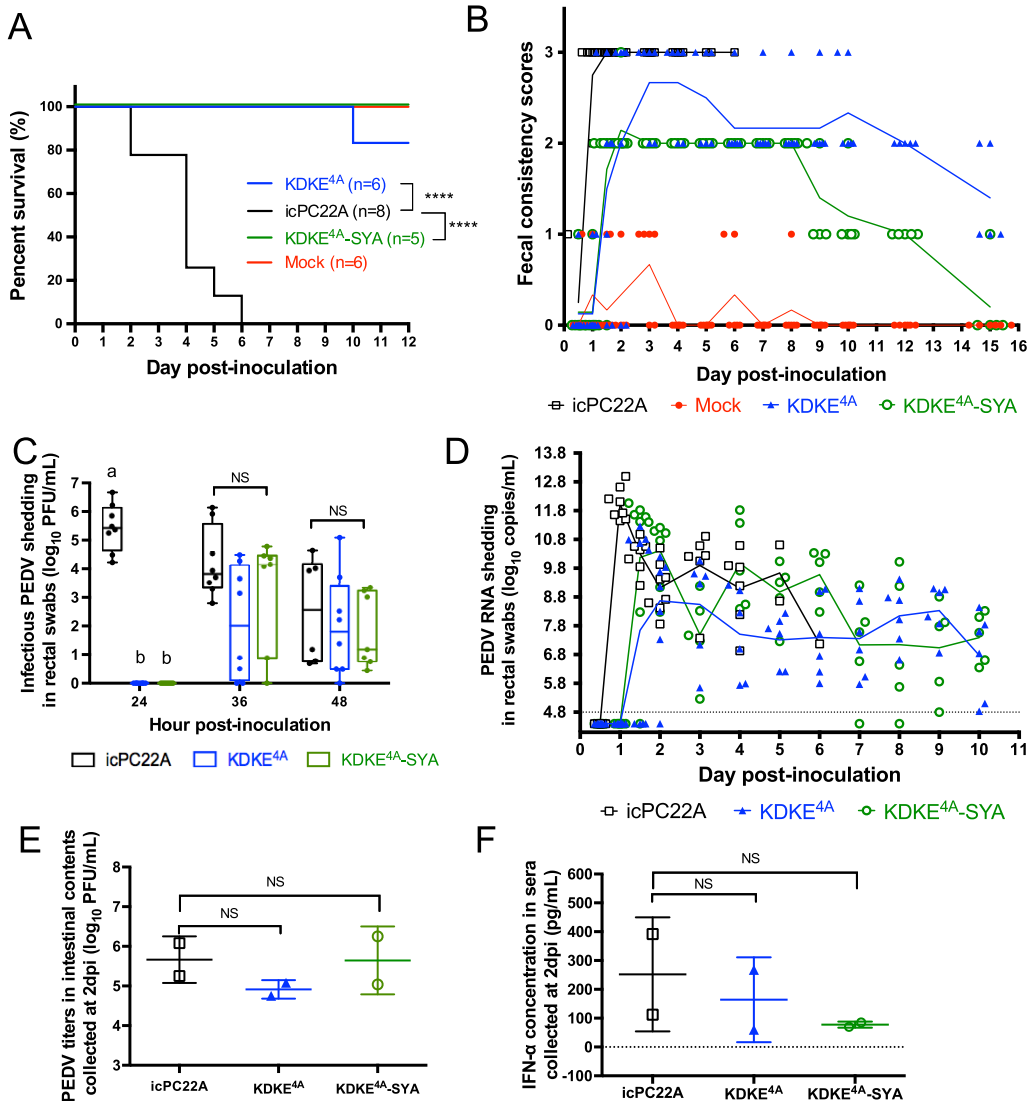


**FIG 4** Pathogenicity of the recombinant PEDVs in Gn piglets. (A) Survival curves. Piglets were monitored within 12 dpi. The data were analyzed by log rank test (\*\*\*\*,  $P < 0.001$ ). Two diarrheic piglets from the KDKE<sup>4A</sup> and KDKE<sup>4A</sup>-SYA groups and one pig from the mock group were euthanized at 2 dpi for histopathological examination and excluded from calculation of mortality rates. (B) Fecal consistency scores of pigs within 16 dpi. Each dot represents the score of an individual pig; each line indicates the mean scores of a group. A pig with a score of  $\geq 2$  was defined as having diarrhea. (C) Infectious PEDV shedding titers in rectal swabs within 48 hpi. Each dot represents the titer of an individual pig; each box represents the interquartile range, the line in the box represents the median, and the whiskers show the range of a group of values. Groups at the same time point with significant differences ( $P < 0.05$ ) are indicated with different letters; NS, not significant. (D) PEDV RNA shedding titers in rectal swabs within 11 dpi. Each symbol represents the titer of the PEDV N gene in 1 ml or gram of rectal swab sample from an individual piglet collected daily; each line indicates the mean values of a group. Values below the detection limit (dotted line at 4.8  $\log_{10}$  copies/ml) were considered negative. (E) Infectious PEDV titers in the small-intestinal contents collected from the pigs that died or were euthanized at 2 dpi. (F) IFN- $\alpha$  concentrations in sera collected from the pigs that died or were euthanized at 2 dpi. (E and F) Values in the mutant groups were compared with those in the virulent-icPC22A group by Student's *t* test (NS, not significant).

verified by Sanger sequencing. No sequence alteration was found in the nine introduced mutations (Fig. 7B). The virus has acquired one synonymous mutation in nsp12, two synonymous mutations in nsp15, and one nonsynonymous (F375L) mutation in the S1 subunit (Fig. 7C). We sequenced the nsp16 and S cytoplasmic tail region from the rectal swab samples from KDKE<sup>4A</sup>-infected ( $n = 5$ ) and KDKE<sup>4A</sup>-SYA-infected ( $n = 5$ ) pigs collected at 16 to 20 dpi and did not find any reversion of the introduced mutations (data not shown). Due to the low PEDV RNA titers (ranging from 5.17 to 8.90  $\log_{10}$  N gene copies/ml) in these rectal swab samples, we were not able to amplify

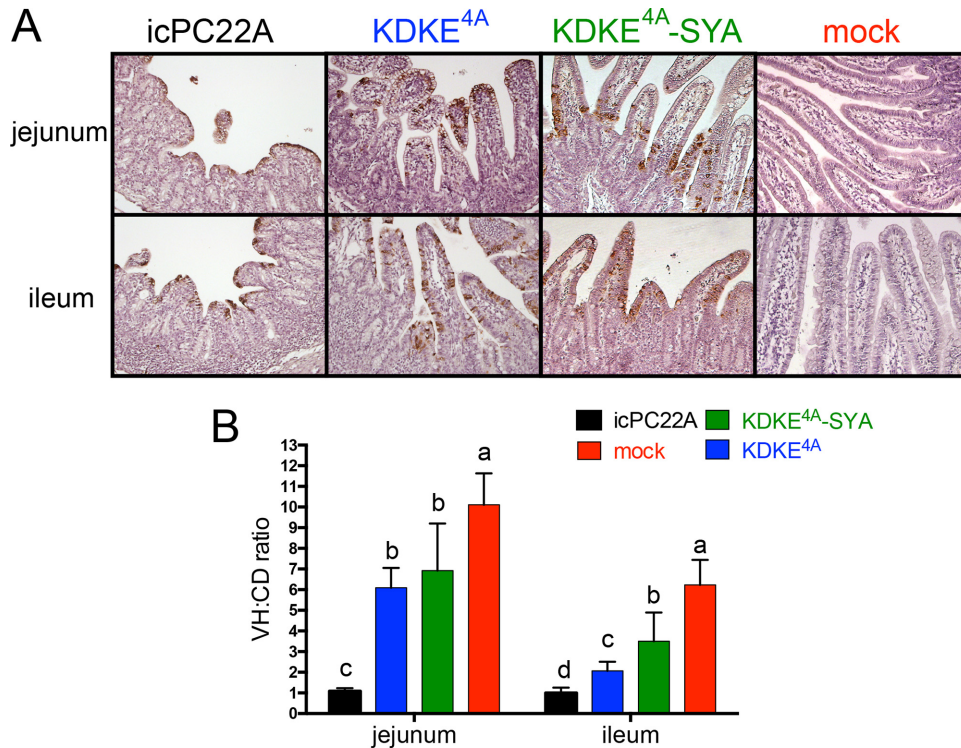


**FIG 5** Histopathological examination of piglets euthanized at 2 dpi. (A) Immunohistochemistry staining of PEDV N proteins (brown signals) in jejunum and ileum sections from piglets (magnification,  $\times 200$ ). (B) VH/CD ratios for piglets. Twenty villi of each intestinal section were measured. Groups with significant differences ( $P < 0.05$ ) are indicated with different letters. The error bars indicate standard deviations.

sufficient amounts for complete genomic sequencing of the mutants. Collectively, these data indicate that the introduced mutations in the catalytic tetrad of PEDV nsp16 and the cytoplasmic tail region in S were stable *in vivo*.

**DISCUSSION**

The emergence and reemergence of enteric CoVs in swine, including PEDV (2), porcine deltacoronavirus (PDCoV) (39), and swine acute diarrhea syndrome (SADS)-CoV (40), have raised concerns about their economic impacts on the global pork industry. Because these CoVs cause clinically similar gastroenteritis but induce no cross-neutralization in pigs (41), it is necessary to develop effective and safe LAVs against each individual CoV. The nsp16 protein of CoVs is highly conserved among CoVs (33), representing a suitable mutagenesis target for this purpose. In the current study, we used PEDV as an example to validate this concept. We evaluated the virulence of recombinant PEDVs bearing the inactivated viral 2'-O-MTase of nsp16 in newborn Gn pigs and characterized their protective efficacies in pigs against challenge with the highly virulent PEDV. By combining the inactivation of nsp16 2'-O-MTase activity and

**TABLE 2** Clinical signs and PEDV shedding in pigs postchallenge with the highly virulent icPC22A (1 to 9 dpc)

Group	No. of pigs	Mortality rate [% (no/total)]	Diarrhea rate [% (no/total)] <sup>a</sup>	Duration (days) of severe diarrhea (FC = 3) <sup>a</sup>	Duration (days) of diarrhea (FC $\geq 2$ ) <sup>a</sup>	Peak mean fecal infectious PEDV shedding titer ( $\log_{10}$ PFU/ml)	Peak mean fecal PEDV N RNA shedding titer ( $\log_{10}$ copies/ml); dpc
KDKE <sup>4A</sup>	5	0 (0/5)B <sup>b</sup>	20 (1/5)B	0.00 $\pm$ 0.00B	0.20 $\pm$ 0.44B	0.04 $\pm$ 0.09B	6.32 $\pm$ 0.52B; 3
KDKE <sup>4A</sup> -SYA	5	0 (0/5)B	0 (0/5)C	0.00 $\pm$ 0.00B	0.00 $\pm$ 0.00B	0.00 $\pm$ 0.00B	5.28 $\pm$ 0.91B; 3
Mock challenge	6	33 (2/6)A	100 (6/6)A	4.50 $\pm$ 2.43A	7.17 $\pm$ 0.98A	2.79 $\pm$ 1.03A	10.29 $\pm$ 0.76A; 3

<sup>a</sup>Fecal consistency (FC) was scored as follows: 0, solid; 1, pasty; 2, semiliquid; and 3, liquid. FC scores of 2 and 3 were considered moderate diarrhea and severe diarrhea, respectively.

<sup>b</sup>Different letters indicate significant differences between groups ( $P < 0.05$ ).

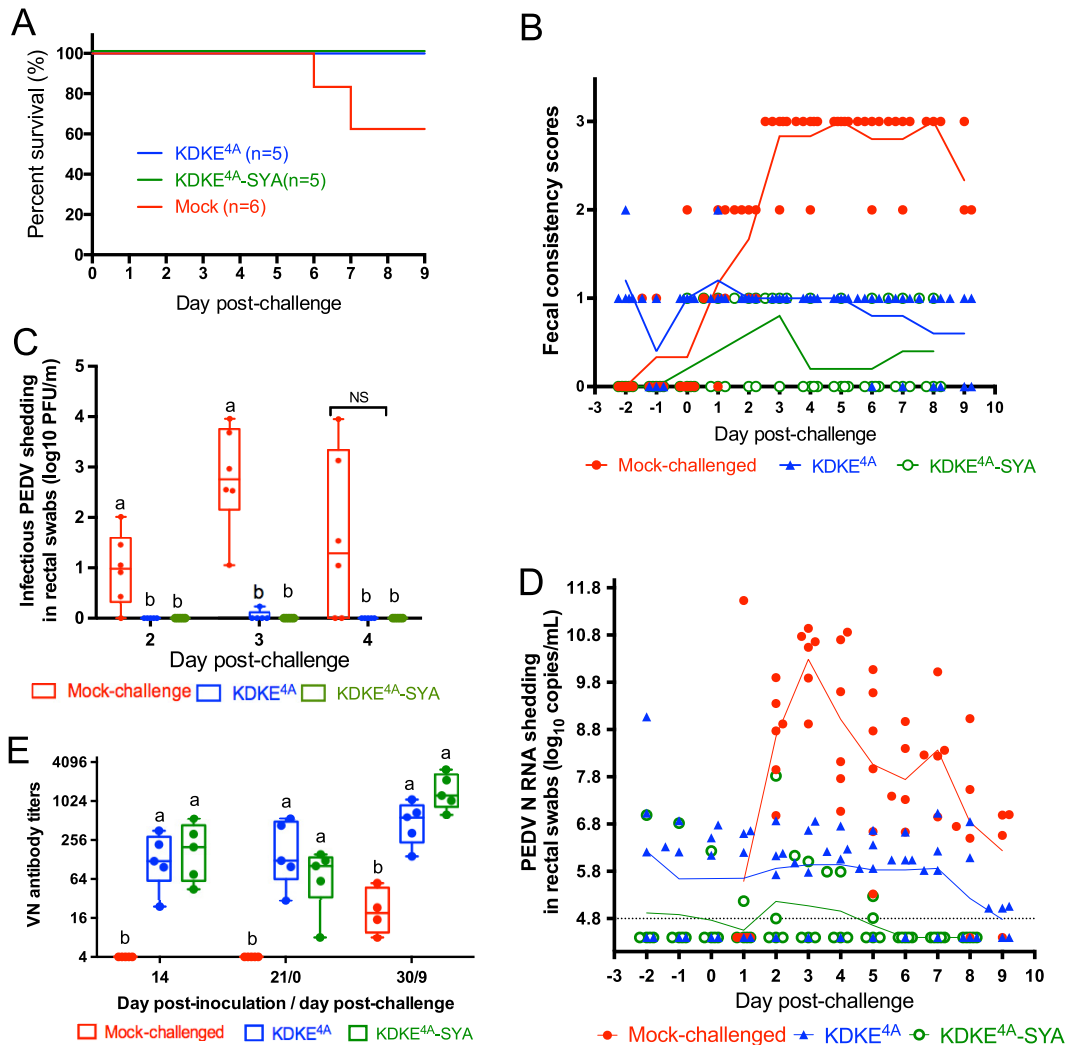


**FIG 6** Induction of cross-protection by nsp16 mutants in Gn pigs against icPC22A challenge. (A) Survival curves of pigs by 9 dpc. (B) Fecal consistency scores of pigs postchallenge. Each dot represents the score of an individual pig; each line indicates the mean scores of a group. A pig with a score of  $\geq 2$  was defined as having diarrhea. (C) Fecal infectious PEDV shedding titers of pigs postchallenge. Each dot represents the titer of an individual pig; each box represents the interquartile range, and the line in the box represents the median; the whiskers show the ranges of a group of values. (D) Fecal PEDV RNA shedding profile of pigs after challenge. Each symbol represents the copies of the N gene in 1 ml or gram of rectal swab sample from an individual piglet; each line indicates the mean values of a group. Values below the detection limit (4.8  $\log_{10}$  copies/ml) were considered negative. (E) VN antibody titers in sera collected at different time points. (C and E) Groups at the same time point with significant differences ( $P < 0.05$ ) are indicated with different letters; NS, not significant.

the endocytosis signal of the S protein, we showed that the KDKE<sup>4A</sup>-SYA mutant was more attenuated and induced better protection than KDKE<sup>4A</sup> against the virulent-PEDV challenge. We also confirmed that the introduced mutations in the KDKE<sup>4A</sup>-SYA genome were stable after passing the mutant virus in Gn pigs three times. Currently, both G1 and G2 PEDV strains are circulating among pigs in different countries. Two subtypes of PEDV are cocirculating in the United States, the highly virulent original U.S. PEDV strains (e.g., PC22A) and the clinically milder S-INDEL PEDV strains (e.g., Iowa106) (42). Previous studies demonstrated that live S-INDEL strains induce partial cross-protection against challenge with the original U.S. PEDV (7, 43), although the two subtypes of PEDV induced similar levels of VN antibodies in serum and their VN antibodies cross-reacted to each other (44). Sera collected in this study also cross-neutralized the S-INDEL strain Iowa106 at the same level in Vero cells (data not shown). Further pig experiments are needed to examine whether the original U.S. PEDV-based KDKE<sup>4A</sup>-SYA mutant induces sufficient protection against challenge with a heterolo-

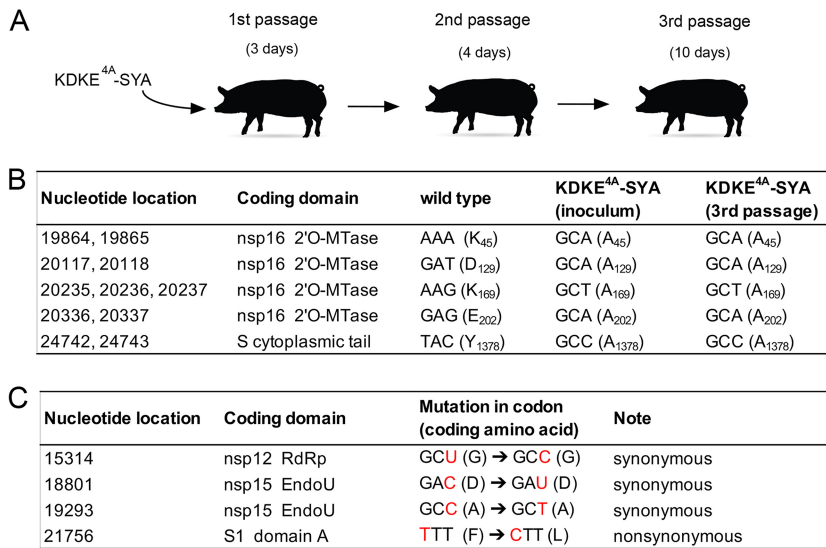


**FIG 7** The introduced mutations in KDKE<sup>4A</sup>-SYA were stable after passaging in pigs successively three times. (A) Experimental design of the *in vivo* passaging. The days of each passage in the pig are indicated. (B) Comparison of the introduced mutations in the KDKE<sup>4A</sup>-SYA genome before (inoculum) and after (3rd passage) passaging three times. The positions of the residues in each viral protein are indicated as subscripts. (C) Mutations occurred in the remaining genome of the 3rd passage of KDKE<sup>4A</sup>-SYA. Additional mutations are marked in red. RdRp, RNA-dependent RNA polymerase; EndoU, endoribonuclease; S1, S1 subunit of the S protein.

gous S-INDEL PEDV strain. However, the original U.S. PEDV strains should be the main target of PEDV LAVs due to their high virulence and prevalence in the field.

The catalytic tetrad K-D-K-E is highly conserved in the 2'-O-MTases of not only the *Coronaviridae*, but also other viral families (45). We showed that, consistent with the attenuated phenotype of similarly engineered CoVs (32–34), flaviviruses (46–48), and paramyxovirus (49), PEDV mutants without 2'-O-MTase activity were attenuated in neonatal Gn piglets and became more vulnerable to innate immune responses (Fig. 2E). The KDKE<sup>4A</sup> mutant harbored four alanine substitutions in the catalytic tetrad, different from the previously reported nsp16-inactivated MHV, SARS-CoV, and MERS-CoV, which contained only one amino acid mutation (D129A or D130D). It has been shown that replacing each of the 4 residues with alanine almost completely abolished the 2'-O-MTase activity of the *Escherichia coli*-expressed, SARS-CoV nsp16 *in vitro* (27, 31). Our study demonstrated for the first time that a CoV lacking all the K-D-K-E residues was still viable both *in vitro* and *in vivo*. This design also improved the safety of this PEDV LAV candidate, because the 2'-O-MTase activity of nsp16 can be restored only when all four alanine substitutions revert to K-D-K-E. The PEDV D129A mutant was not evaluated in pigs because we speculate that the single mutant might be more virulent than the KDKE<sup>4A</sup> mutant, similar to the observations for the D130A mutants of SARS-CoV and MERS-CoV (32, 33). Unlike the SARS-CoV and MERS-CoV D130A mutants, which replicated equivalently to the wild type, the KDKE<sup>4A</sup> mutant replicated to lower titers (Fig. 2A and B and 3A) and generated smaller plaques (Fig. 2D) than the parental icPC22A virus in Vero cells. One potential reason is that the K-D-K-E residues may have other, unknown functions in viral replication. It is also possible that the PEDV D129A mutant may still retain marginal 2'-O-MTase activity, whereas the KDKE<sup>4A</sup> mutant may have completely lost this enzymatic activity. Substantial evidence to support this point can be obtained by quantification of the percentage of 2'-O-methylated viral RNAs between the mutants using radioactive-labeling approaches. The less efficient replication of KDKE<sup>4A</sup> or KDKE<sup>4A</sup>-SYA in Vero cells may be a drawback for the large-scale production of PEDV LAVs. This issue can be overcome by using engineered cell lines that can support effective replication of the mutants. It has been reported that the replication of the MHV D129A mutant was also poor in wild-type macrophages but was enhanced

in interferon-induced protein with tetratricopeptide repeats 1 (IFIT 1)-knockout macrophages (34). Alternatively, stable expression of wild-type nsp16 in a cell line may compensate for the inactivated catalytic tetrad function in the mutants and restore virus propagation *in vitro*, although this cell line may facilitate the reversion of nsp16-inactivated mutants *in vitro*.

Similar to infection with other enteric RNA viruses (50, 51), PEDV infection elicits both type I and type III IFNs that trigger innate immune responses in pigs. IFN- $\alpha$  and - $\beta$  secreted by various immune and epithelial cells are known to induce antiviral effects systemically but do not act to clear enteric viral pathogens or restrict their replication in epithelial cells. In contrast, IFN- $\lambda$ 1, - $\lambda$ 3, and - $\lambda$ 4 are mainly produced by epithelial cells and activate antiviral responses at mucosal sites (37, 38). However, several studies have reported that PEDV-infected epithelial cell lines did not express significantly increased amounts of type I and type III IFNs in the early stage of infection (usually within 12 to 24 h) (37, 52–55), probably due to inhibition by multiple viral proteins. So far, it has been determined that at least 10 PEDV proteins suppress IFN production, including nsp1, nsp3, nsp5, nsp7, nsp14, nsp15, ORF3, E, M, and N (37, 52, 53, 56–58). For instance, inactivation of nsp15 (endoribonuclease) of a PEDV reduced its IFN antagonism, resulting in enhanced induction of both type I and type III IFNs *in vitro* and viral attenuation *in vivo* (53). In the present study, we also observed similar results for PEDV mutants with inactivated nsp16. These mutants triggered earlier IFN responses than icPC22A in IPEC-DQ cells, probably due to the 2'-O-methylation-free viral RNAs that triggered sensor molecule melanoma differentiation-associated protein 5 (MDA5). Inoculation with KDKE<sup>4A</sup> and KDKE<sup>4A</sup>-SYA did not induce higher levels of IFN- $\alpha$  in the sera of pigs euthanized at 2 dpi (Fig. 4F), which was likely due to the much more robust replication of the virulent icPC22A than of the two mutants *in vivo*. We could not determine the local IFN responses in the intestinal tissues, due to no pigs being euthanized at an early time point, e.g., within 24 hpi. Based on the study of Vero cell-adapted PEDV LAV (20), the level of host immune response correlates with the efficiency of viral replication in the intestines. The tendency to induce stronger local IFN responses at the early stage of infection by the nsp16-inactivated PEDV mutants may contribute to the overall immunogenicity, although the viruses replicate less robustly *in vivo*. Further investigation of infection with these PEDV mutants in pigs or porcine enteroid cultures may discover detailed mechanisms.

Compared with KDKE<sup>4A</sup>, the KDKE<sup>4A</sup>-SYA double mutant displayed a higher level of attenuation in piglets and induced better (100%) protection from diarrhea postchallenge with a high dose of the highly virulent PEDV icPC22A. The double mutant may induce improved immune responses in pigs, potentially due to the combined effects of the KDKE<sup>4A</sup> and icYA mutants. The Y1378A mutation in the cytoplasmic tail of the S protein not only inactivates the endocytosis signal YEVF, but also disrupts the 6-nucleotide TRS of the ORF3 sgRNA by 2 nucleotides (Fig. 1D), resulting in decreased synthesis of sgRNA-3 in the infected cells (36). Since PEDV ORF3 protein is an IFN antagonist (37, 52), the icYA mutant also induced higher type I and type III IFN responses than icPC22A in IPEC-DQ cells (Fig. 3). Moreover, the inactivated endocytosis signal enhances the formation of syncytia, which may facilitate the spread of the KDKE<sup>4A</sup>-SYA mutant between cells during the early stage of infection. We observed that the KDKE<sup>4A</sup>-SYA mutant replicated to slightly higher titers than the KDKE<sup>4A</sup> mutant at 1.5 dpi in piglets (Table 1 and Fig. 4D). The lack of this endocytosis signal increases the amount of S proteins being presented on the surfaces of the infected enterocytes, contributing to better T cell activation (36). Future studies on cellular immune responses to these mutants in pigs are warranted to increase understanding of the mechanisms of the enhanced attenuation and better immunity of KDKE<sup>4A</sup>-SYA than of KDKE<sup>4A</sup>.

Maintaining the genetic stability of CoV LAV candidates is critical for vaccine development. Recombinant CoVs with mutations in certain viral proteins are unstable *in vivo*. For example, after serial passaging in BALB/c mice for 20 days (10 times), a recombinant SARS-CoV lacking the entire E protein (SARS-CoV- $\Delta$ E) acquired an addi-

tional PDZ-binding motif (PBM) in the accessory protein 8a that compensated for the loss of the same motif in the E protein (59). In contrast, the catalytic tetrad in CoV nsp16 seems to be a stable target for mutagenesis. The SARS-CoV D130A mutant retained the two nucleotide substitutions in nsp16 after continuous replication in immune-deficient mice for 30 days (35). Similarly, we also showed that the nine nucleotide substitutions were stable in nsp16 of the *in vivo*-passaged KDKE<sup>4A</sup>-SYA (Fig. 7) and in fecal samples collected at 16 to 20 dpi from the KDKE<sup>4A</sup>- or KDKE<sup>4A</sup>-SYA-infected pigs. After the three passages in pigs (total, 17 days), the genome of the KDKE<sup>4A</sup>-SYA mutant acquired one additional amino acid substitution in the S1 subunit and three synonymous mutations in nsp12 and nsp15 (Fig. 7C). However, it is unlikely that the mutated S protein can compensate for the missing 2'-O-MTase activity of this PEDV mutant, but it would be interesting to evaluate the pathogenesis of the *in vivo*-passaged virus in pigs in the future. Notably, compared with young pigs, older animals have more mature immune systems and can induce stronger selective pressure for the introduced mutation. It is also necessary to evaluate the genetic stability of KDKE<sup>4A</sup>-SYA in adult pigs in the future.

Another approach to prevent potential reversion to virulent CoV is to introduce mutations in multiple genes with different functions. Under certain selective pressures *in vivo*, a mutation in one gene may revert to wild type, but an additional mutation may still be preserved and retain the attenuation. Also, two independent recombination events are required to revert two distant mutations to wild type when the LAV and a virulent virus coinfect a cell. One study showed that combined inactivation of nsp16 and nsp14 further reduced the reversion to virulence of the recombinant SARS-CoV *in vivo* (35). A similar effect was also observed in other recombinant SARS-CoVs with combined deletions in nsp1 and the E protein (59). In our study, combined mutations were made for KDKE<sup>4A</sup> in nsp16 and endocytosis signal (Y1378A) in S. Interestingly, the removal of this endocytosis signal has occurred naturally in the S genes of Vero cell-adapted or field PEDV strains (36), suggesting that it is stable for PEDV replication *in vivo* and *in vitro*. Collectively, our data suggest that the engineered KDKE<sup>4A</sup>-SYA mutant was genetically stable in pigs.

Vaccination regimens, including vaccine doses, boosting, use of adjuvants, and timing, determine the efficacy of a PEDV LAV in PEDV-naive pigs. Neonatal piglets are not appropriate targets for PEDV vaccination due to rapid disease development and death in the first week of life. They are protected by acquiring PEDV-neutralizing antibodies via colostrum and milk from sows. Thus, stimulation of sufficient lactogenic immune responses in sows is the key to PEDV vaccination. In this study, we inoculated 4-day-old piglets with 100 PFU/pig of virulent icPC22A (equivalent to 100 to 1,000 median diarrhea doses [PDD<sub>50</sub>]) (60) or the mutants. The dose for oral immunization of sows may likely need to be increased, due to age-related decreased susceptibility (61, 62) and potential preexisting PEDV antibodies in older animals. The immunogenicity of KDKE<sup>4A</sup> and/or KDKE<sup>4A</sup>-SYA mutants in pregnant sows also needs to be evaluated in the future. A recent study demonstrated that intramuscular inoculation of a virulent PEDV triggered intestinal infection in pigs (63), suggesting that oral vaccination may be combined with other routes to establish a better primary infection in the intestines of sows. Use of PEDV booster vaccines can be adapted from previous TGEV and rotavirus studies, in which administration of subunit or inactivated vaccines as boosters improved the efficacies of the oral LAVs (64, 65). Vitamin A and probiotics have been demonstrated to be effective adjuvants for rotavirus vaccines in pigs (66, 67). Moreover, the timing of vaccination significantly affects multiple immune parameters in sows. A recent study showed that PEDV infection in the second trimester of gestation stimulated the strongest protective immune responses in gilts compared with gilts inoculated in the first or third trimester (68).

In conclusion, we developed and evaluated a PEDV LAV candidate by combining inactivated 2'-O-MTase with an abolished endocytosis signal in the S protein. This mutant PEDV replicated less effectively but induced stronger type I and type III IFN responses in cell culture. Our data illustrate that this strategy is a safe and effective

approach to developing LAVs against PEDV, as well as potentially other swine enteric CoVs.

## MATERIALS AND METHODS

**Cells, plasmids, and reagents.** Vero cells (ATCC number CCL81) were cultured in Dulbecco's modified Eagle's medium (DMEM) (Gibco, Carlsbad, CA) supplemented with 5% fetal bovine serum (FBS) and antibiotics/antimycotics (Gibco, Carlsbad, CA). IPEC-DQ is a subclone of the swine intestinal epithelial cell line IPEC-J2, which was generated previously (37). IPEC-DQ cells were cultured in RPMI 1640 (Gibco, Carlsbad, CA) supplemented with 10% FBS. The propagation of PEDV in Vero cells was described previously. After PEDV adsorption, the cells were maintained in DMEM or RPMI 1640 supplemented with 0.3% tryptose phosphate broth (TPB) (Sigma-Aldrich, St. Louis, MO) and 10  $\mu$ g/ml trypsin (Gibco, Carlsbad, CA). Recombinant human IFN- $\beta$  was purchased from PBL Assay Science (Piscataway Township, NJ). The sensitivity of Vero cells to the human IFN- $\beta$  pretreatment was validated in previous reports (32). The coding sequences of wild-type nsp16 and nsp16 with the D129A or KDKE<sup>4A</sup> mutation were cloned into the pXJ41 vector as described previously (52).

**Dual-luciferase reporter assay.** The wild-type IFN- $\lambda$ 1 luciferase reporter construct [p-55 $\lambda$ 1-(−225/−36)-Luc], the IFN- $\beta$  luciferase reporter construct, and the assay were described previously (37, 52). The *Renilla* luciferase plasmid pRL-TK (Promega) was included as an internal control. Briefly, IPEC-DQ cells were grown in a 24-well plate at 70% confluence and transfected with the IFN- $\lambda$ 1- or IFN- $\beta$ -luciferase plasmid (0.3  $\mu$ g/well) and pRL-TK (0.03  $\mu$ g/well) for 24 h. The cells were then infected with the PEDV mutants at an MOI of 1. Cell lysates were harvested at 0, 9, and 12 hpi, and luciferase activities were determined using a dual-luciferase reporter assay system (Promega, Madison, WI). Signals were obtained with a luminometer (Wallac 1420 Victor multilabel counter; Perkin Elmer, Waltham, MA).

**Structural modeling and sequence alignment.** The 3D structure of PEDV nsp16 was modeled with the SWISS-MODEL (<https://swissmodel.expasy.org>) online tool using SARS-CoV nsp16 as the template (27). The structure alignment of SARS-CoV and PEDV nsp16 was performed by using the RCSB PDB protein comparison tool (<https://www.rcsb.org>).

**Generation of mutant PEDVs from cDNA clones.** A set of five plasmids encoding the full-length genomic cDNA of PEDV strain PC22A (GenBank accession no. KY499262) was generated previously (22). The point mutations were introduced into the wild-type plasmid using NEBuilder HiFi DNA assembly master mix (NEB, Ipswich, MA). All the plasmids were verified by Sanger sequencing. The recovery of the recombinant PEDVs from infectious cDNA clones was described previously (69). The plasmids were digested, purified, and mixed together in equal molar ratio. The full-length genomic cDNA was ligated with T4 ligase (NEB, Ipswich, MA) and transcribed into RNA using an mMessage mMachine T7 transcription kit (Ambion, Austin, CA, USA). The genomic RNA was mixed with PEDV N gene transcripts and electroporated into Vero cells cultured in medium supplemented with trypsin. After transfection, cytopathic effects (CPE) appeared within 2 days. The P0 viruses were harvested and subjected to plaque purification. A single clone of each PEDV mutant was propagated once in Vero cells to generate a viral stock (P1). The full-length genome of each virus stock was verified by Sanger sequencing. Additionally, the recombinant PEDV icYA bearing only the Y1378A mutation in the genome was generated previously (36) and was included in this study as a control.

**Study design of the experimental infection of Gn pigs.** All the animal experiments in this study were approved by the Institutional Animal Care and Use Committee (IACUC) of The Ohio State University. Gn piglets were derived from two PEDV-naive sows. A total of 29 piglets were randomly divided into four groups, and 3 or 4 piglets in the same group were housed in one isolator, as described previously (70). At 4 days of age, Gn piglets were orally inoculated with recombinant PEDV KDKE<sup>4A</sup> ( $n = 8$ ; 100 PFU/pig), KDKE<sup>4A</sup>-SYA ( $n = 7$ ; 100 PFU/pig), or icPC22A ( $n = 8$ ; 100 PFU/pig) or mock inoculated ( $n = 7$ ; phosphate-buffered saline [PBS]). The dose of PEDV corresponds to 100 to 1,000 PDD<sub>50</sub> of the PC22A strain in 4-day-old cesarean-derived, colostrum-deprived piglets, as titrated by us previously (60). Two diarrheic piglets in the KDKE<sup>4A</sup> and KDKE<sup>4A</sup>-SYA groups and one mock-treated piglet were euthanized at 2 dpi for histopathological examination and were excluded from the calculation of mortality rates. At 21 dpi, each surviving pig was challenged orally with 6 log<sub>10</sub> PFU of icPC22A and housed for 9 more days to evaluate protection. We observed clinical signs, including diarrhea, vomiting, and anorexia. Rectal swabs were collected daily with two additional time points at 12 and 36 hpi (hours postchallenge [hpc]). The severity of diarrhea was scored based on the fecal consistency in individual pigs: 0, solid; 1, pasty; 2, semiliquid (mild diarrhea); and 3, liquid (severe diarrhea). The virus and viral RNA shedding titers in the rectal swab samples were determined by plaque assay and reverse transcription-quantitative PCR (RT-qPCR), respectively, as described previously (71, 72). Peripheral blood samples were collected at 14 dpi, 21 dpi (1 h before challenge), and 30 dpi (9 days postchallenge) to monitor the serum antibody titers. Histopathological examinations, including IHC staining of PEDV N antigens in jejunum and ileum tissues, were performed. Viral neutralizing antibody assays were performed as reported previously (43). Following our IACUC protocol, any moribund piglets that showed anorexia and dehydration over 24 h had to be euthanized based on the instructions of institutional veterinarians.

**ELISA for IFN- $\alpha$  detection.** The enzyme-linked immunosorbent assay (ELISA) for IFN- $\alpha$  detection was described previously (68, 73). Briefly, Nunc Maxisorp 96-well plates were coated with anti-porcine IFN- $\alpha$  (2.5 mg/ml; clone K9; R&D Systems, Minneapolis, MN) at 37°C overnight. Biotinylated anti-porcine IFN- $\alpha$  (3.75 mg/ml; clone F17; R&D Systems, Minneapolis, MN) was used for detection. The plates were developed, and cytokine concentrations were calculated based on the standard curve. The detection limit for the IFN- $\alpha$  assay is 4 pg/ml.

**Evaluation of genetic stability of introduced mutations in the KDKE<sup>4A</sup>-SYA.** To serially passage the mutant in Gn pigs, the small-intestinal contents (SIC) of a 4-day-old KDKE<sup>4A</sup>-SYA (the P1 virus)-infected pig euthanized at 3 dpi were collected. A second PEDV-naive piglet at 10 days of age was inoculated with the diluted SIC containing 100 PFU of the P1 virus. At 4 dpi, the piglet was euthanized, and the SIC were collected (P2 virus). A third PEDV-naive piglet at 17 days of age was inoculated with the diluted SIC containing 1,000 PFU of the P2 virus. At 10 dpi, the third piglet was euthanized, and the SIC were collected. Total RNA of the SIC was extracted using an RNeasy minikit (Qiagen, Germany). The total cDNA was generated by reverse transcription using a Super Script III kit (Invitrogen, Carlsbad, CA). PCR fragments covering the complete PEDV genome were amplified using PrimeStar HiFi polymerase (TaKaRa, Japan).

To confirm the stability of the mutations in the recombinant PEDV KDKE<sup>4A</sup>- and KDKE<sup>4A</sup>-SYA- infected pigs, the coding sequences of nsp16 and the S cytoplasmic tail were amplified from the rectal swab samples collected at 16 to 20 dpi by reverse transcription followed by nested PCR using PrimeStar HiFi polymerase (TaKaRa, Japan). The Sanger sequencing was performed by the Genomics Shared Resource at The Ohio State University.

**Plaque assay and growth curves.** For plaque assay, monolayers of Vero cells were inoculated with 10-fold serially diluted recombinant PEDVs for 1 h in the presence of trypsin (10  $\mu$ g/ml). Then, the inocula were removed and the Vero cells were washed twice with PBS. The cells were overlaid with agarose-minimal essential medium (MEM) mixture supplemented with trypsin and TPB. The growth curves of PEDV in Vero cells were determined by inoculation of monolayers of cells with each of the recombinant PEDVs at an MOI of 0.005 or 1. After 1 h of adsorption, the inocula were removed, and the cell monolayers were washed twice with PBS. Maintenance medium containing trypsin and TPB was added to the cell culture. The total number of viruses (intracellular and extracellular) of each sample was determined after freezing and thawing the cultures once at appropriate time points. The infectious titers of viral samples were determined by plaque assays. The growth curve of PEDV in IPEC-DQ cells (MOI = 1) was determined by a similar procedure and titrated by the TCID<sub>50</sub> method.

**IFN- $\beta$  sensitivity assay.** Vero cells were cultured in medium supplemented with different concentrations of IFN- $\beta$  for 18 h prior to PEDV inoculation. After removal of the medium and washing the cells with PBS three times, the cells were inoculated with recombinant PEDVs at an MOI of 0.01 and cultured for an additional 24 h. The supernatants and cells were frozen at  $-80^{\circ}\text{C}$ . After freezing and thawing once, the samples of one PEDV mutant collected at different time points were titrated simultaneously by plaque assays.

**RNA isolation, reverse transcription, and real-time RT-qPCR.** For gRNA and sgmRNA detection, Vero cells were inoculated with recombinant PEDVs at an MOI of 1 for 10 h. Total cellular RNA was isolated using an RNeasy minikit (Qiagen, Germany). Positive-sense viral RNA was reverse transcribed with gene-specific reverse primers using Moloney murine leukemia virus (MMLV) reverse transcriptase (Promega, Madison, WI). The cDNA was subjected to quantitative PCR using TaqMan qPCR reagents (Qiagen, Germany). The gRNA was amplified with forward primer (TGAAGCCGTCATCACTATTCTG), reverse primer (AATCCCTCAACAGTGTCAGC), and probe (6-carboxyfluorescein [FAM]-TGCAATGCCGTTTC GTGTCCTTC-black hole quencher [BHQ]). sgmRNA-N was amplified with forward primer (CTCTTGCTAC TCAATTCAACTAAACAGAAAC), reverse primer (CCAGTATCCAATTTGCTGTGCC), and probe (FAM-TCAGGATCGTGCCGCAAAC-BHQ). sgmRNA-3 was amplified with forward primer (CTATCTACGGATAGTTAGTCC), reverse primer (CTGTGTCAATCGTGATTG), and probe (FAM-ACATCACTGCACGTGGAC-BGH). Copy numbers of each amplicon were determined by standard curves and normalized with the mass of total cellular RNA. sgmRNA-N was also detected in the sample as a control. Both sgmRNAs are reported as copies per  $10^8$  copies of gRNA. For cellular IFN mRNA detection, IPEC-DQ cells were inoculated with recombinant PEDVs at an MOI of 1. Total cellular RNA was isolated, and cellular DNA was removed by treating the RNA with DNase I (Qiagen). One microgram of total RNA was reverse transcribed using MMLV reverse transcriptase and random primers. The cDNA was subjected to quantitative PCR using SYBR green PCR mix (Life Technologies, Carlsbad, CA) according to the manufacturer's instructions. The primer sequences were described previously (37, 52). The  $\beta$ -actin gene was used as an internal control. The threshold cycle ( $C_T$ ) values for target genes and the differences in their  $C_T$  values ( $\Delta C_T$ ) were determined. Relative transcription levels of target genes are presented as fold changes relative to the respective controls using the  $2^{-\Delta\Delta C_T}$  threshold method (74).

**Statistical analysis.** Statistical analyses were performed using GraphPad Prism 6.0. The data in Fig. 4C and 6C and E are shown in box-and-whisker plots with individual values. Comparisons of means of groups in these figures, the tables, and Fig. 2C and E and 5B were analyzed by one-way analysis of variance (ANOVA) followed by Tukey's multiple-comparison test. Groups at the same time point with significant differences ( $P < 0.05$ ) are indicated by different letters. The data in Fig. 2B, F, H, and G and 3 were analyzed by one-way ANOVA followed by Dunnett's multiple-comparison test by comparing each group with the icPC22A group at the same time point. The data in Fig. 4E and F were analyzed by Student's  $t$  test by comparing each mutant group with the icPC22A group. The data in Fig. 4A and 6A were analyzed by log rank test.

## ACKNOWLEDGMENTS

This project was supported by Agriculture and Food Research Initiative Competitive Grants no. 2015-67015-23067 (Q.W., principal investigator [PI]; L.J.S., co-PI) and no. 2018-67015-28287 (D.Y., PI) from the National Institute of Food and Agriculture, U.S. Department of Agriculture.

We thank Juliette Hanson, Ronna Wood, Megan Strother, Sara Tallmadge, Dennis Hartzler, and Jeff Ogg for animal care assistance and Xiaohong Wang and Tianfei Yu for technical assistance. We are grateful to Eric Nelson at South Dakota State University for providing us the mouse monoclonal antibodies against PEDV N proteins. We thank Chang-Won Lee and Scott Kenney for their critical reviews of the manuscript.

## REFERENCES

- Sun RQ, Cai RJ, Chen YQ, Liang PS, Chen DK, Song CX. 2012. Outbreak of porcine epidemic diarrhea in suckling piglets, China. *Emerg Infect Dis* 18:161–163. <https://doi.org/10.3201/eid1801.111259>.
- Stevenson GW, Hoang H, Schwartz KJ, Burrough ER, Sun D, Madson D, Cooper VL, Pillatzki A, Gauger P, Schmitt BJ, Koster LG, Killian ML, Yoon KJ. 2013. Emergence of porcine epidemic diarrhea virus in the United States: clinical signs, lesions, and viral genomic sequences. *J Vet Diagn Invest* 25:649–654. <https://doi.org/10.1177/1040638713501675>.
- Puranaveja S, Poolperm P, Lertwatcharasarakul P, Kesdaengsakonwut S, Boonsoongnern A, Urairong K, Kitikoon P, Choojai P, Kedkovid R, Teankum K, Thanawongnuwech R. 2009. Chinese-like strain of porcine epidemic diarrhea virus, Thailand. *Emerg Infect Dis* 15:1112–1115. <https://doi.org/10.3201/eid1507.081256>.
- Schulz LL, Tonsor GT. 2015. Assessment of the economic impacts of porcine epidemic diarrhea virus in the United States. *J Animal Sci* 93:5111–5118. <https://doi.org/10.2527/jas.2015-9136>.
- Paarlberg PL. 2014. Updated estimated economic welfare impacts of porcine epidemic diarrhea virus (PEDV). <http://ageconsearch.umn.edu/bitstream/174517/2/14-4.Updated%20Estimated%20Economic%20Welfare%20Impacts%20of%20PEDV.pdf>.
- Bjstrom-Kraft J, Woodard K, Giménez-Lirola L, Setness B, Ji J, Lasley P, Nelson E, Zhang J, Baum D, Gauger P, Main R, Zimmerman J. 2018. Serum and mammary secretion antibody responses in porcine epidemic diarrhea-immune gilts following porcine epidemic diarrhea vaccination. *J Swine Health Prod* 26:34–40.
- Opriessnig T, Gerber PF, Shen H, de Castro A, Zhang J, Chen Q, Halbur P. 2017. Evaluation of the efficacy of a commercial inactivated genogroup 2b-based porcine epidemic diarrhea virus (PEDV) vaccine and experimental live genogroup 1b exposure against 2b challenge. *Vet Res* 48:69. <https://doi.org/10.1186/s13567-017-0472-z>.
- Crawford K, Lager KM, Kulshreshtha V, Miller LC, Faaberg KS. 2016. Status of vaccines for porcine epidemic diarrhea virus in the United States and Canada. *Virus Res* 226:108–116. <https://doi.org/10.1016/j.virusres.2016.08.005>.
- Langel SN, Paim FC, Lager KM, Vlasova AN, Saif LJ. 2016. Lactogenic immunity and vaccines for porcine epidemic diarrhea virus (PEDV): historical and current concepts. *Virus Res* 226:93–107. <https://doi.org/10.1016/j.virusres.2016.05.016>.
- Chattha KS, Roth JA, Saif LJ. 2015. Strategies for design and application of enteric viral vaccines. *Annu Rev Anim Biosci* 3:375–395. <https://doi.org/10.1146/annurev-animal-022114-111038>.
- Song D, Moon H, Kang B. 2015. Porcine epidemic diarrhea: a review of current epidemiology and available vaccines. *Clin Exp Vaccine Res* 4:166–176. <https://doi.org/10.7774/cevr.2015.4.2.166>.
- Jarvis MC, Lam HC, Zhang Y, Wang L, Hesse RA, Hause BM, Vlasova A, Wang Q, Zhang J, Nelson MI, Murtaugh MP, Marthaler D. 2016. Genomic and evolutionary inferences between American and global strains of porcine epidemic diarrhea virus. *Prev Vet Med* 123:175–184. <https://doi.org/10.1016/j.prevetmed.2015.10.020>.
- Jie T, Benqiang L, Jinghua C, Ying S, Huili L. 2018. Preparation and characterization of an attenuated porcine epidemic diarrhea virus strain by serial passaging. *Arch Virol* 163:2997–3004. <https://doi.org/10.1007/s00705-018-3968-6>.
- Lin C-M, Hou Y, Marthaler DG, Gao X, Liu X, Zheng L, Saif L, Wang Q. 2017. Attenuation of an original US porcine epidemic diarrhea virus strain PC22A via serial cell culture passage. *Vet Microbiol* 201:62–71. <https://doi.org/10.1016/j.vetmic.2017.01.015>.
- Li Y, Wang G, Wang J, Man K, Zhang Q. 2017. Cell attenuated porcine epidemic diarrhea virus strain Zhejiang08 provides effective immune protection attributed to dendritic cell stimulation. *Vaccine* 35: 7033–7041. <https://doi.org/10.1016/j.vaccine.2017.10.052>.
- Chang Y-C, Kao C-F, Chang C-Y, Jeng C-R, Tsai P-S, Pang V, Chiou H-Y, Peng J-Y, Cheng I-C, Chang H-W. 2017. Evaluation and comparison of the pathogenicity and host immune responses induced by a G2b Taiwan porcine epidemic diarrhea virus (strain Pintung 52) and its highly cell-culture passaged strain in conventional 5-week-old pigs. *Viruses* 9:121. <https://doi.org/10.3390/v9050121>.
- Lee S, Son K-Y, Noh Y-H, Lee S-C, Choi H-W, Yoon I-J, Lee C. 2017. Genetic characteristics, pathogenicity, and immunogenicity associated with cell adaptation of a virulent genotype 2b porcine epidemic diarrhea virus. *Vet Microbiol* 207:248–258. <https://doi.org/10.1016/j.vetmic.2017.06.019>.
- Kim Y, Oh C, Shivanna V, Hesse RA, Chang KO. 2017. Trypsin-independent porcine epidemic diarrhea virus US strain with altered virus entry mechanism. *BMC Vet Res* 13:356. <https://doi.org/10.1186/s12917-017-1283-1>.
- Chen F, Zhu Y, Wu M, Ku X, Ye S, Li Z, Guo X, He Q. 2015. Comparative genomic analysis of classical and variant virulent parental/attenuated strains of porcine epidemic diarrhea virus. *Viruses* 7:5525–5538. <https://doi.org/10.3390/v7102891>.
- Lin C-M, Ghimire S, Hou Y, Boley P, Langel SN, Vlasova AN, Saif LJ, Wang Q. 2019. Pathogenicity and immunogenicity of attenuated porcine epidemic diarrhea virus PC22A strain in conventional weaned pigs. *BMC Vet Res* 15:26. <https://doi.org/10.1186/s12917-018-1756-x>.
- Zuñiga S, Pascual-Iglesias A, Sanchez CM, Sola I, Enjuanes L. 2016. Virulence factors in porcine coronaviruses and vaccine design. *Virus Res* 226:142–151. <https://doi.org/10.1016/j.virusres.2016.07.003>.
- Hou Y, Lin CM, Yokoyama M, Yount BL, Marthaler D, Douglas AL, Ghimire S, Qin Y, Baric RS, Saif LJ, Wang Q. 2017. Deletion of a 197-amino-acid region in the N-terminal domain of spike protein attenuates porcine epidemic diarrhea virus in piglets. *J Virol* 91:e00227-17. <https://doi.org/10.1128/JVI.00227-17>.
- Baker SC. 2010. Coronavirus: molecular biology, p 445–453. In Mahy BWJ, van Regenmortel MHV (ed), *Desk encyclopedia of general virology*. Academic Press, New York, NY.
- Hyde JL, Diamond MS. 2015. Innate immune restriction and antagonism of viral RNA lacking 2-O methylation. *Virology* 479–480:66–74. <https://doi.org/10.1016/j.virol.2015.01.019>.
- Daffis S, Szretter KJ, Schriewer J, Li J, Youn S, Errett J, Lin T-Y, Schneller S, Züst R, Dong H, Thiel V, Sen GC, Fensterl V, Klimstra WB, Pierson TC, Buller RM, Gale M, Shi P-Y, Diamond MS. 2010. 2'-O methylation of the viral mRNA cap evades host restriction by IFIT family members. *Nature* 468:452–456. <https://doi.org/10.1038/nature09489>.
- Decroly E, Imbert I, Coutard B, Bouvet M, Selisko B, Alvarez K, Gorbalenya AE, Snijder EJ, Canard B. 2008. Coronavirus nonstructural protein 16 is a cap-0 binding enzyme possessing (nucleoside-2'-O)-methyltransferase activity. *J Virol* 82:8071–8084. <https://doi.org/10.1128/JVI.00407-08>.
- Chen Y, Su C, Ke M, Jin X, Xu L, Zhang Z, Wu A, Sun Y, Yang Z, Tien P, Ahola T, Liang Y, Liu X, Guo D. 2011. Biochemical and structural insights into the mechanisms of SARS coronavirus RNA ribose 2'-O-methylation by nsp16/nsp10 protein complex. *PLoS Pathog* 7:e1002294. <https://doi.org/10.1371/journal.ppat.1002294>.
- Chen Y, Cai H, Pan J, Xiang N, Tien P, Ahola T, Guo D. 2009. Functional screen reveals SARS coronavirus nonstructural protein nsp14 as a novel cap N7 methyltransferase. *Proc Natl Acad Sci U S A* 106:3484–3489. <https://doi.org/10.1073/pnas.0808790106>.
- Ma Y, Wu L, Shaw N, Gao Y, Wang J, Sun Y, Lou Z, Yan L, Zhang R, Rao Z. 2015. Structural basis and functional analysis of the SARS coronavirus nsp14-nsp10 complex. *Proc Natl Acad Sci U S A* 112:9436–9441. <https://doi.org/10.1073/pnas.1508686112>.
- Bouvet M, Lugari A, Posthuma CC, Zevenhoven JC, Bernard S, Betzi S, Imbert I, Canard B, Guillemot J-C, Lécine P, Pfefferle S, Drosten C, Snijder EJ, Decroly E, Morelli X. 2014. Coronavirus nsp10, a critical co-factor for activation of multiple replicative enzymes. *J Biol Chem* 289: 25783–25796. <https://doi.org/10.1074/jbc.M114.577353>.
- Decroly E, Debarnot C, Ferron F, Bouvet M, Coutard B, Imbert I, Gluais L,

- Papageorgiou N, Sharff A, Bricogne G, Ortiz-Lombardia M, Lescar J, Canard B. 2011. Crystal structure and functional analysis of the SARS-coronavirus RNA cap 2'-O-methyltransferase nsp10/nsp16 complex. *PLoS Pathog* 7:e1002059. <https://doi.org/10.1371/journal.ppat.1002059>.
32. Menachery VD, Yount BL, Josset L, Gralinski LE, Scobey T, Agnihothram S, Katze MG, Baric RS. 2014. Attenuation and restoration of severe acute respiratory syndrome coronavirus mutant lacking 2'-O-methyltransferase activity. *J Virol* 88:4251–4264. <https://doi.org/10.1128/JVI.03571-13>.
  33. Menachery VD, Gralinski LE, Mitchell HD, Dinnon KH, Leist SR, Yount BL, Graham RL, McAnarney ET, Stratton KG, Cockrell AS, Debbink K, Sims AC, Waters KM, Baric RS. 2017. Middle East respiratory syndrome coronavirus nonstructural protein 16 is necessary for interferon resistance and viral pathogenesis. *mSphere* 2:e00346-17. <https://doi.org/10.1128/mSphere.00346-17>.
  34. Züst R, Cervantes-Barragan L, Habjan M, Maier R, Neuman BW, Ziebuhr J, Szretter KJ, Baker SC, Barchet W, Diamond MS, Siddell SG, Ludewig B, Thiel V. 2011. Ribose 2'-O-methylation provides a molecular signature for the distinction of self and non-self mRNA dependent on the RNA sensor Mda5. *Nat Immunol* 12:137–143. <https://doi.org/10.1038/ni.1979>.
  35. Menachery VD, Gralinski LE, Mitchell HD, Dinnon KH, Leist SR, Yount BL, McAnarney ET, Graham RL, Waters KM, Baric RS. 2018. Combination attenuation offers strategy for live attenuated coronavirus vaccines. *J Virol* 92:e00710-18. <https://doi.org/10.1128/JVI.00710-18>.
  36. Hou Y, Meulia T, Gao X, Saif LJ, Wang Q. 2019. Deletion of both the tyrosine-based endocytosis signal and the endoplasmic reticulum retrieval signal in the cytoplasmic tail of spike protein attenuates porcine epidemic diarrhea virus in pigs. *J Virol* 93:e01758-18. <https://doi.org/10.1128/JVI.01758-18>.
  37. Zhang Q, Ke H, Blikslager A, Fujita T, Yoo D. 2017. Type III interferon restriction by porcine epidemic diarrhea virus and the role of viral protein nsp1 in IRF1 signaling. *J Virol* 92:e01677-17. <https://doi.org/10.1128/JVI.01677-17>.
  38. Li L, Fu F, Xue M, Chen W, Liu J, Shi H, Chen J, Bu Z, Feng L, Liu P. 2017. IFN- $\lambda$  preferably inhibits PEDV infection of porcine intestinal epithelial cells compared with IFN- $\alpha$ . *Antiviral Res* 140:76–82. <https://doi.org/10.1016/j.antiviral.2017.01.012>.
  39. Wang L, Byrum B, Zhang Y. 2014. Detection and genetic characterization of deltacoronavirus in pigs, Ohio, USA, 2014. *Emerg Infect Dis* 20:1227–1230. <https://doi.org/10.3201/eid2007.140296>.
  40. Zhou P, Fan H, Lan T, Yang X-L, Shi W-F, Zhang W, Zhu Y, Zhang Y-W, Xie Q-M, Mani S, Zheng X-S, Li B, Li J-M, Guo H, Pei G-Q, An X-P, Chen J-W, Zhou L, Mai K-J, Wu Z-X, Li D, Anderson DE, Zhang L-B, Li S-Y, Mi Z-Q, He T-T, Cong F, Guo P-J, Huang R, Luo Y, Liu X-L, Chen J, Huang Y, Sun Q, Zhang X-L-L, Wang Y-Y, Xing S-Z, Chen Y-S, Sun Y, Li J, Daszak P, Wang L-F, Shi Z-L, Tong Y-G, Ma J-Y. 2018. Fatal swine acute diarrhoea syndrome caused by an HKU2-related coronavirus of bat origin. *Nature* 556:255–258. <https://doi.org/10.1038/s41586-018-0010-9>.
  41. Wang Q, Vlasova AN, Kenney SP, Saif LJ. 2019. Emerging and re-emerging coronaviruses in pigs. *Curr Opin Virol* 34:39–49. <https://doi.org/10.1016/j.coviro.2018.12.001>.
  42. Oka T, Saif LJ, Marthaler D, Esseili MA, Meulia T, Lin C-M, Vlasova AN, Jung K, Zhang Y, Wang Q. 2014. Cell culture isolation and sequence analysis of genetically diverse US porcine epidemic diarrhea virus strains including a novel strain with a large deletion in the spike gene. *Vet Microbiol* 173:258–269. <https://doi.org/10.1016/j.vetmic.2014.08.012>.
  43. Lin C-M, Annamalai T, Liu X, Gao X, Lu Z, El-Tholoth M, Hu H, Saif LJ, Wang Q. 2015. Experimental infection of a US spike-insertion deletion porcine epidemic diarrhea virus in conventional nursing piglets and cross-protection to the original US PEDV infection. *Vet Res* 46:134. <https://doi.org/10.1186/s13567-015-0278-9>.
  44. Chen Q, Thomas JT, Giménez-Lirola LG, Hardham JM, Gao Q, Gerber PF, Opriessnig T, Zheng Y, Li G, Gauger PC, Madson DM, Magstadt DR, Zhang J. 2016. Evaluation of serological cross-reactivity and cross-neutralization between the United States porcine epidemic diarrhea virus prototype and 5-INDEL-variant strains. *BMC Vet Res* 12:70. <https://doi.org/10.1186/s12917-016-0697-5>.
  45. Feder M, Pas J, Wyrwicz LS, Bujnicki JM. 2003. Molecular phylogenetics of the RrmJ/fibrillarin superfamily of ribose 2'-O-methyltransferases. *Gene* 302:129–138. [https://doi.org/10.1016/S0378-1119\(02\)01097-1](https://doi.org/10.1016/S0378-1119(02)01097-1).
  46. Ray D, Shah A, Tilgner M, Guo Y, Zhao Y, Dong H, Deas TS, Zhou Y, Li H, Shi P-Y. 2006. West Nile virus 5'-cap structure is formed by sequential guanine N-7 and ribose 2'-O methylations by nonstructural protein 5. *J Virol* 80:8362–8370. <https://doi.org/10.1128/JVI.00814-06>.
  47. Li S-H, Dong H, Li X-F, Xie X, Zhao H, Deng Y-Q, Wang X-Y, Ye Q, Zhu S-Y, Wang H-J, Zhang B, Leng Q-B, Zuest R, Qin E-D, Qin C-F, Shi P-Y. 2013. Rational design of a flavivirus vaccine by abolishing viral RNA 2'-O methylation. *J Virol* 87:5812–5819. <https://doi.org/10.1128/JVI.02806-12>.
  48. Züst R, Dong H, Li RX, Chang DC, Zhang B, Balakrishnan T, Toh YX, Jiang T, Li SH, Deng YQ, Ellis BR, Ellis EM, Poidinger M, Zolezzi F, Qin CF, Shi PY, Fink K. 2013. Rational design of a live attenuated dengue vaccine: 2'-O-methyltransferase mutants are highly attenuated and immunogenic in mice and macaques. *PLoS Pathog* 9:e1003521. <https://doi.org/10.1371/journal.ppat.1003521>.
  49. Zhang Y, Wei Y, Zhang X, Cai H, Niewiesk S, Li J. 2014. Rational design of human metapneumovirus live attenuated vaccine candidates by inhibiting viral mRNA cap methyltransferase. *J Virol* 88:11411–11429. <https://doi.org/10.1128/JVI.00876-14>.
  50. Pott J, Mahlaköiv T, Mordstein M, Duerr CU, Michiels T, Stockinger S, Staeheli P, Hornef MW. 2011. IFN- $\lambda$  determines the intestinal epithelial antiviral host defense. *Proc Natl Acad Sci U S A* 108:7944–7949. <https://doi.org/10.1073/pnas.1100552108>.
  51. Swamy M, Abeler-Dörner L, Chettle J, Mahlaköiv T, Goubau D, Chakravarty P, Ramsay G, Reis e Sousa C, Staeheli P, Blacklaws BA, Heeney JL, Hayday AC. 2015. Intestinal intraepithelial lymphocyte activation promotes innate antiviral resistance. *Nat Commun* 6:7090. <https://doi.org/10.1038/ncomms8090>.
  52. Zhang Q, Shi K, Yoo D. 2016. Suppression of type I interferon production by porcine epidemic diarrhea virus and degradation of CREB-binding protein by nsp1. *Virology* 489:252–268. <https://doi.org/10.1016/j.virol.2015.12.010>.
  53. Deng X, van Geelen A, Buckley AC, O'Brien A, Pillatzki A, Lager KM, Faaberg KS, Baker SC. 2019. Coronavirus endoribonuclease activity in porcine epidemic diarrhea virus suppresses type I and type III interferon responses. *J Virol* 93:e02000-18. <https://doi.org/10.1128/JVI.02000-18>.
  54. Cao L, Ge X, Gao Y, Herrler G, Ren Y, Ren X, Li G. 2015. Porcine epidemic diarrhea virus inhibits dsRNA-induced interferon- $\beta$  production in porcine intestinal epithelial cells by blockade of the RIG-I-mediated pathway. *Virology* 12:127. <https://doi.org/10.1186/s12985-015-0345-x>.
  55. Guo L, Luo X, Li R, Xu Y, Zhang J, Ge J, Bu Z, Feng L, Wang Y. 2016. Porcine epidemic diarrhea virus infection inhibits interferon signaling by targeted degradation of STAT1. *J Virol* 90:8281–8292. <https://doi.org/10.1128/JVI.01091-16>.
  56. Xu X, Zhang H, Zhang Q, Dong J, Liang Y, Huang Y, Liu H-J, Tong D. 2013. Porcine epidemic diarrhea virus E protein causes endoplasmic reticulum stress and up-regulates interleukin-8 expression. *Virology* 10:26. <https://doi.org/10.1186/1743-422X-10-26>.
  57. Ding Z, Fang L, Jing H, Zeng S, Wang D, Liu L, Zhang H, Luo R, Chen H, Xiao S. 2014. Porcine epidemic diarrhea virus nucleocapsid protein antagonizes beta interferon production by sequestering the interaction between IRF3 and TBK1. *J Virol* 88:8936–8945. <https://doi.org/10.1128/JVI.00700-14>.
  58. Wang D, Fang L, Shi Y, Zhang H, Gao L, Peng G, Chen H, Li K, Xiao S. 2016. Porcine epidemic diarrhea virus 3C-like protease regulates its interferon antagonism by cleaving NEMO. *J Virol* 90:2090–2101. <https://doi.org/10.1128/JVI.02514-15>.
  59. Jimenez-Guardeño JM, Regla-Nava JA, Nieto-Torres JL, DeDiego ML, Castaño-Rodríguez C, Fernandez-Delgado R, Perlman S, Enjuanes L. 2015. Identification of the mechanisms causing reversion to virulence in an attenuated SARS-CoV for the design of a genetically stable vaccine. *PLoS Pathog* 11:e1005215. <https://doi.org/10.1371/journal.ppat.1005215>.
  60. Liu X, Lin C-M, Annamalai T, Gao X, Lu Z, Esseili MA, Jung K, El-Tholoth M, Saif LJ, Wang Q. 2015. Determination of the infectious titer and virulence of an original US porcine epidemic diarrhea virus PC22A strain. *Vet Res* 46:109. <https://doi.org/10.1186/s13567-015-0249-1>.
  61. Jung K, Annamalai T, Lu Z, Saif LJ. 2015. Comparative pathogenesis of US porcine epidemic diarrhea virus (PEDV) strain PC21A in conventional 9-day-old nursing piglets vs. 26-day-old weaned pigs. *Vet Microbiol* 178:31–40. <https://doi.org/10.1016/j.vetmic.2015.04.022>.
  62. Thomas JT, Chen Q, Gauger PC, Giménez-Lirola LG, Sinha A, Harmon KM, Madson DM, Burrough ER, Magstadt DR, Salzbrenner HM, Welch MW, Yoon K-J, Zimmerman JJ, Zhang J. 2015. Effect of porcine epidemic diarrhea virus infectious doses on infection outcomes in naïve conventional neonatal and weaned pigs. *PLoS One* 10:e0139266. <https://doi.org/10.1371/journal.pone.0139266>.
  63. Chen P, Wang K, Hou Y, Li H, Li X, Yu L, Jiang Y, Gao F, Tong W, Yu H, Yang Z, Tong G, Zhou Y. 2019. Genetic evolution analysis and pathogenicity assessment of porcine epidemic diarrhea virus strains circulating

- in part of China during 2011-2017. *Infect Genet Evol* 69:153-165. <https://doi.org/10.1016/j.meegid.2019.01.022>.
64. Azevedo MP, Vlasova AN, Saif LJ. 2013. Human rotavirus virus-like particle vaccines evaluated in a neonatal gnotobiotic pig model of human rotavirus disease. *Expert Rev Vaccines* 12:169-181. <https://doi.org/10.1586/erv.13.3>.
  65. Park S, Sestak K, Hodgins DC, Shoup DI, Ward LA, Jackwood DJ, Saif LJ. 1998. Immune response of sows vaccinated with attenuated transmissible gastroenteritis virus (TGEV) and recombinant TGEV spike protein vaccines and protection of their suckling pigs against virulent TGEV challenge exposure. *Am J Vet Res* 59:1002-1008.
  66. Kandasamy S, Chattha KS, Vlasova AN, Saif LJ. 2014. Prenatal vitamin A deficiency impairs adaptive immune responses to pentavalent rotavirus vaccine (RotaTeq) in a neonatal gnotobiotic pig model. *Vaccine* 32: 816-824. <https://doi.org/10.1016/j.vaccine.2013.12.039>.
  67. Kandasamy S, Vlasova AN, Fischer D, Kumar A, Chattha KS, Rauf A, Shao L, Langel SN, Rajashekara G, Saif LJ. 2016. Differential effects of *Escherichia coli* Nissle and *Lactobacillus rhamnosus* strain GG on human rotavirus binding, infection, and B cell immunity. *J Immunol* 196: 1780-1789. <https://doi.org/10.4049/jimmunol.1501705>.
  68. Langel SN, Paim FC, Alhamo MA, Buckley A, Van Geelen A, Lager KM, Vlasova AN, Saif LJ. 2019. Stage of gestation at porcine epidemic diarrhea virus infection of pregnant swine impacts maternal immunity and lactogenic immune protection of neonatal suckling piglets. *Front Immunol* 10:727. <https://doi.org/10.3389/fimmu.2019.00727>.
  69. Beall A, Yount B, Lin C-M, Hou Y, Wang Q, Saif L, Baric R. 2016. Characterization of a pathogenic full-length cDNA clone and transmission model for porcine epidemic diarrhea virus strain PC22A. *mBio* 7:e01451-15. <https://doi.org/10.1128/mBio.01451-15>.
  70. Saif LJ, Ward LA, Yuan L, Rosen BI, To TL. 1996. The gnotobiotic piglet as a model for studies of disease pathogenesis and immunity to human rotaviruses, p 153-161. *In* Chiba S, Estes MK, Nakata S, Calisher CH (ed), *Gnotobiotic piglets and human rotaviruses*. Springer, New York, NY.
  71. Jung K, Wang Q, Scheuer KA, Lu Z, Zhang Y, Saif LJ. 2014. Pathology of US porcine epidemic diarrhea virus strain PC21A in gnotobiotic pigs. *Emerg Infect Dis* 20:662.
  72. Su Y, Hou Y, Wang Q. 2019. The enhanced replication of an S-intact PEDV during coinfection with an S1 NTD-del PEDV in piglets. *Vet Microbiol* 228:202-212. <https://doi.org/10.1016/j.vetmic.2018.11.025>.
  73. Miyazaki A, Kandasamy S, Michael H, Langel SN, Paim FC, Chepngeno J, Alhamo MA, Fischer DD, Huang H-C, Srivastava V, Kathayat D, Deblais L, Rajashekara G, Saif LJ, Vlasova AN. 2018. Protein deficiency reduces efficacy of oral attenuated human rotavirus vaccine in a human infant fecal microbiota transplanted gnotobiotic pig model. *Vaccine* 36: 6270-6281. <https://doi.org/10.1016/j.vaccine.2018.09.008>.
  74. Livak KJ, Schmittgen TD. 2001. Analysis of relative gene expression data using real-time quantitative PCR and the  $2^{-\Delta\Delta CT}$  method. *Methods* 25:402-408. <https://doi.org/10.1006/meth.2001.1262>.